ISSN 0381 - 4319

National Research Council Canada
Conseil national de recherches Canada

FIRE RESISTANCE OF REINFORCED CONCRETE COLUMNS

by T.T. Lie, T.D. Lin, D.E. Allen, M.S. Abrams

DBR Paper No. 1167
Division of Building Research

Price $3.25

Canada OTTAWA NRCC 23065

NATIONAL RESEARCH COUNCIL CANADA

DIVISION OF BUILDING RESEARCH

FIRE RESISTANCE OF REINFORCED CONCRETE COLUMNS

by

T.T. Lie, T.D. Lin, D.E. Allen, M.S. Abrams

Ottawa

February 1984

FIRE RESISTANCE OF REINFORCED CONCRETE COLUMNS

by

T.T. Lie, T.D. Lin, D.E. Allen and M.S. Abrams

Studies on columns were started a few years ago for the purpose of updating the fire resistance ratings for reinforced concrete columns in the National Building Code of Canada [1,2]. These ratings were related to full scale test results obtained in about 1920. Since that time design procedures have changed and the safety factor has decreased. This indicates a need for revision of these ratings.

Facilities for testing columns have been constructed recently at the National Research Council of Canada. Using these facilities it is possible to study experimentally the influence of the various factors that determine the fire resistance of columns. It is also possible to validate the mathematical models that have been developed for predicting the fire resistance of reinforced concrete columns.

The present study was an extension of the previous studies [1,2], and was undertaken in cooperation with the Portland Cement Association. Its main objectives were:

1) To generate fire resistance data on reinforced concrete columns designed in accordance with current ACI 318-77 or CSA-CAN A23.3-M77 Building Codes.
2) To develop general methods for the calculation of the fire resistance of concrete columns and walls for a wide range of applications.

PROGRAM

The National Research Council and the Portland Cement Association have jointly worked out a multi-phase program for the study of the behaviour of full size reinforced concrete columns exposed to fire. The study variables in the program include the following:

1. load intensity
2. eccentricity of loading
3. fire exposure intensity
4. cross-section of column or wall
5. column height
6. thickness of concrete cover
7. amount of steel
8. type of aggregate
9. strength of concrete
10. moisture content of concrete
11. restraining effect, and possibly
12. unsymmetrical fire exposure.

A computer program written by NRC prior to the start of the joint research program, is capable of simulating these conditions. By comparing calculated results with those obtained during testing, the validity of the mathematical model can be verified.

This report deals with the first phase of the program, which involved the testing of twelve columns. The columns were designed and manufactured by PCA in Skokie, Illinois. The specimens were transported by truck to the Fire Research laboratories of the National Research Council of Canada, where the fire tests were conducted. The objectives of the first phase of the program were to:

1. prove out the new column testing facility, including all control and recording equipment and obtain information on the characteristics of the furnace;
2. establish the methods of fabricating the columns, installing them in the furnace and loading them;
3. obtain the information necessary for the design of the rest of the program;
4. collect information on the influence on fire resistance of load, cross-section, moisture and aggregate, for prediction of the fire resistance of columns and walls;
5. compare experimental and calculated temperatures, deformations and fire resistance of the reinforced concrete columns.

TEST SPECIMENS

In the first phase of the study program a series of twelve tied, reinforced concrete columns were fabricated and tested. Ten of the columns had a cross-section of 305 × 305 mm (12 × 12 in.), one of 203 × 203 mm (8 × 8 in.) and one of 406 × 406 mm (16 × 16 in.). All columns were 3810 mm (12 ft 6 in.) long. Three specimens were made with carbonate aggregate and nine with siliceous.

Table I gives details of cross-section, the type of aggregate used in the concrete, the relative humidity measured in the centre of the column at the time of the test and the concrete cylinder strength measured at different times.

Materials

Details concerning materials used in the fabrication of the specimens are given below:

Cement: Type I, a general purpose cement for construction of reinforced concrete structures, was used.

Aggregate: Carbonate sand and gravel were from Elgin, Illinois. Siliceous sand and gravel were from Eau Claire, Wisconsin. The maximum size of the aggregate was 19 mm (3/4 in.). The petrographic information, given in Tables II and III, was obtained following the procedures of ASTM C295-65

[3]. Sieve analyses were conducted. Gradation curves for the two aggregates are shown in Figs. 1 and 2. Other information needed for proportioning the mix, such as specific gravity, moisture content, unit weight, and fineness modulus of the aggregates, is listed in Table IV.

Steel: Deformed bars meeting requirements of ASTM Designation: A615-80 [4] were used for main and tie bars. The longitudinal steel bars in the columns were 20M (No. 6) and 25M (No. 8), and the ties were 10M (No. 3). A tensile test was performed for each bar size to determine yield and ultimate strength. The test results are listed in Table V.

Concrete Mix: Several trial mixes for determining optimum proportions were made to produce a 34.5 MPa (5000 psi) strength non-air-entrained concrete. A water/cement ratio of 0.6 was used for the carbonate aggregate concrete and 0.5 for the siliceous aggregate concrete. Batch quantities and measured properties of fresh concrete are given in Table VI.

The average 28-day concrete strengths were 33.8 MPa (4896 psi) for carbonate aggregate concrete and 34.2 MPa (4958 psi) for siliceous aggregate concrete. The individual 28-day strengths of the cylinders are given in Table I.

Fabrication

The columns were cast in specially designed forms. The reinforcement cage was assembled by welding the longitudinal bars to a steel end plate. Chromel-alumel thermocouples were secured to the reinforcing steel at specified locations after the cage was properly positioned in the form. In order to avoid any possible dislocation of the thermocouples during casting, a careful working plan was followed as described below.

Reinforcing bars and steel plates

The column length was 3810 mm (12 ft 6 in.) measured from end plate to end plate. The longitudinal reinforcing bars were cut to 3800 mm (12 ft 5 1/2 in.). The bars were machined at both ends, for a length of 19 mm (3/4 in.) for the 203 and 305 mm (8 and 12 in.) columns to a diameter of 12.7 mm (1/2 in.), and 19 mm, respectively. The bars of the 406 mm (16 in.) column were machined for a length of 31.8 mm (1 1/4 in.) to a diameter of 19 mm. Fig. 3 shows details of the finished bars. A micrometer was used to measure the diameters of the machined segments.

The dimensions of the end plates were 863 × 863 × 38 mm (34 × 34 × 1 1/2 in.) for the 406 mm (16 in.) square column and 533 × 533 × 25 mm (21 × 21 × 1 in.) for the 203 and 305 mm (8 and 12 in.) square columns. Holes 20.6 mm (13/16 in.) in diameter, spaced to accommodate the longitudinal bars, were drilled through the plates.

The main bars and ties were tied together to complete the steel cage. The cage then was placed vertically on a levelled end plate in such a way that the machined segments of the bars were positioned in the holes.

Welding

The provisions of AWS Designation D12.1-75 [5] were followed when welding plates and bars. These members were preheated with a propane torch to 288°C (550°F), to prevent brittle failure during welding. The side fillet weld was done around bars on the inner face of the bottom plate. McKay E10018-D2 and DYTRON-579 welding rods were used. Both types of welding rods have tensile strength of 834.9 MPa (121 000 psi). Mild-steel welding rods were used to fill up the 6 mm (1/4 in.) deep holes on the outer faces of the plate. The rough surfaces of the welded joints on the outer face of the plate were ground to a smooth finish.

The welding of the top steel plate was performed after the casting of the columns. Before positioning the top plate a 6 mm (1/4 in.) layer of mortar was spread over the top of the column to ensure good contact between steel plate and concrete. The mortar was made of 1 part cement and 3 parts siliceous sand. Using the same procedure as for the bottom plate, the top plate was welded on the outer side to the bars and smoothed.

Forms

Forms were made for the 203 mm (8 in.), 305 mm (12 in.) and 406 mm (16 in.) square columns. At the start of casting the front side of the form was left open for depositing fresh concrete. Plywood window pieces were bolted to the form to close the opening as casting progressed upwards.

Thermocouples

Butt-welded chromel-alumel thermocouples with a thickness of 0.912 mm (0.0359 in.) were used to make thermocouple frames for measuring concrete temperatures at several locations in different cross-sections of the columns. Each frame consisted of a number of thermocouples tied to steel rods that were firmly secured to the main reinforcing bars. Temperatures were measured at one-quarter height, at mid-height and at three-quarter height of the column. At mid-height the temperatures were measured along the whole length of an axis and a diagonal of the section; at the other two levels the temperatures were measured only along half of the axis and half of the diagonal of the section. The locations of the thermocouples in the concrete are shown in Fig. 4.

In addition, a number of thermocouples were mounted on the reinforcing steel bars and ties. The locations of the thermocouples on the steel are shown in Fig. 5 and in more detail in Figs. 6, 7 and 8.

Concrete Placement

Concrete was mixed in a 0.17 m^3 (6 ft^3) tilting drum mixer. Shovels and scoops were used to deposit concrete in the form. A small internal vibrator was carefully applied to consolidate the concrete. As casting progressed upward, the window pieces were successively closed and tightly bolted to the form to avoid possible moisture leaks. The top surface of the column was screeded and finished with a small wood float.

Lifting hooks were embedded on opposite sides of the specimen at 800 mm (2 ft 7 1/2 in.) from the top of the column. A humidity well was positioned at mid-point for measuring relative humidity at mid-depth of the column.

Curing

Concrete was cured under damp burlap for 7 days at 21 to 24°C (70 to 75°F). Forms were then stripped, and columns conditioned in an atmosphere controlled at 21 to 24°C and 30 to 40% relative humidity.

Four columns, tested at a near-oven-dry condition, were kiln-dried at about 93°C (200°F) and 0 to 5% relative humidity. They were removed from the kiln periodically to cool at 23°C (73°F) so that the relative humidity in the concrete could be measured. After the designated moisture condition was reached, the columns were wrapped in plastic to prevent change in their moisture content. In calculations, the moisture content of those columns in near-dry condition was assumed to be 0%. The moisture content of those columns in equilibrium with the atmospheric moisture was assumed to be 5% by volume.

LOAD AND FIRE EXPOSURE CONDITIONS

In determining the conditions, such as load, its application, and fire intensity, under which the fire performance of columns are to be studied, several approaches can be followed. The fire performance can be examined for:

1) maximum loading conditions determined in accordance with ACI 318-77 [6] or CSA-CAN A23.3-M77 [7];
2) standard fire test conditions according to ASTM-E119 [8] or ULC-S101 [9];
3) conditions assumed in the mathematical model for the calculation of fire resistance of the columns;
4) conditions that occur in actual practice.

The factors that determined the different conditions considered in the first phase of this study, are given in Table VII. They include the assumptions with regard to load and its application, column length and material properties, and fire temperature.

In the second column of the table the conditions specified in ACI-318 [6] or CSA-CAN A23.3 [7] are given. The conditions that occur in actual practice during a fire (column 5) are assumed to be equal to these conditions, with the exception of loads. Whereas all loads (dead, live, wind loads, etc.) are taken into account in conventional design of structural members, for actual fire conditions, usually only the dead and part of the live load are present during the fire. All other loads, such as wind or earthquake, may be neglected. In the third column the standard fire test conditions, according to ASTM-E119 [8] or ULC-S101 [9], are given. These conditions differ from those in actual practice in respect to load application and fire temperature. In the standard fire test a concentric

load is applied, whereas in practice there is always some eccentricity of loading. A minimum is specified for structural design in ACI or CSA codes. The other difference is that in the test the fire temperature increases continuously according to a standardized relation, whereas in actual practice it can follow numerous courses, including a period of temperature rise and decay.

In the fourth column the conditions assumed in the mathematical model for calculation of the fire resistance of the columns are shown. The conditions were selected to resemble as closely as possible conditions during the fire test, with regard to load, column end conditions and material properties. In the first phase of the study, only exposure to the standard fire, described in ASTM-E119 [8] or ULC-S101 [9] was considered.

CALCULATION PROCEDURE

The calculation of the fire performance of the columns is carried out in various steps. It involves the calculation of the temperatures in the column, and its deformations and strength during the exposure to fire.

Temperatures of Column

The column temperatures are calculated by a finite difference method [10]. This method has been previously applied to the calculation of temperatures in square reinforced concrete columns [1]. Because the method of deriving the heat transfer equations and calculating the temperatures is described in detail in those studies, it will not be discussed here; only the equations used for calculation of the column temperatures, and information not dealt with in previous studies, will be given.

Division of cross-section into elements

The cross-sectional area of the column is subdivided into a number of elements, arranged in a triangular network (Fig. 9). The elements are square inside the column and triangular at the surface. For the inside elements, the temperature at the centre is taken as representative of the entire element. For the triangular surface elements, the representative points are located on the centre of each hypotenuse.

Because only columns with square cross-sections (and four axes of symmetry) will be considered, it is possible to calculate the temperature distribution in only one-eighth of the cross-sectional area of the column. As illustrated in Fig. 9, in an x-z coordinate system, a point $P_{m,n}$ has the coordinates $x = (m-1)\Delta\xi/\sqrt{2}$ and $z = (n-1)\Delta\xi/\sqrt{2}$.

Equations for the fire/concrete boundary

It will be assumed that the columns are exposed on all sides to the heat of a fire whose temperature course follows that of the standard fire described in ASTM-E119 [8] or ULC-S101 [9]. This temperature course can be approximately described by the following expression:

$$T_f^j = 20 + 750\ (1-\exp(-3.79553\sqrt{\tau})) + 170.41\sqrt{\tau} \qquad (1)$$

where τ is the time in hours and T_f^j is the fire temperature in °C at time $\tau = j\Delta\tau$. (A list of nomenclature used in equations is given in Appendix A.)

The temperature rise in each element can be derived by making a heat balance for them. For a surface element the temperature at a time $\tau = (j+1)\Delta\tau$ is given by the expression:

$$T_{1,n}^{j+1} = T_{1,n}^{j} + \frac{2\Delta\tau}{\left[(\rho_c c_c)_{1,n}^{j} + \rho_w c_w \phi_{1,n}^{j}\right](\Delta\xi)^2}$$

$$\left\{\left(\frac{k_{2,(n-1)}^{j} + k_{1,n}^{j}}{2}\right)\left(T_{2,(n-1)}^{j} - T_{1,n}^{j}\right) + \left(\frac{k_{2,(n+1)}^{j} + k_{1,n}^{j}}{2}\right)\right.$$

$$\left.(T_{2,(n+1)}^{j} - T_{1,n}^{j}) + \sqrt{2}\,\Delta\xi\sigma\varepsilon_f\varepsilon_c\left[(T_f^j + 273)^4 - (T_{1,n}^j + 273)^4\right]\right\}. \qquad (2)$$

Equations for inside the concrete

For the elements in the concrete, the temperature rise at the time $\tau = (j+1)\Delta\tau$ is given by:

$$T_{m,n}^{j+1} = T_{m,n}^{j} + \frac{\Delta\tau}{\left[(\rho_c c_c)_{m,n}^{j} + \rho_w c_w \phi_{m,n}^{j}\right](\Delta\xi)^2}$$

$$\left\{\left(\frac{k_{(m-1),(n-1)}^{j} + k_{m,n}^{j}}{2}\right)\left(T_{(m-1),(n-1)}^{j} - T_{m,n}^{j}\right) + \left(\frac{k_{(m+1),(n-1)}^{j} + k_{m,n}^{j}}{2}\right)\right.$$

$$\left(T_{(m+1),(n-1)}^{j} - T_{m,n}^{j}\right) + \left(\frac{k_{(m-1),(n+1)}^{j} + k_{m,n}^{j}}{2}\right)\left(T_{(m-1),(n+1)}^{j} - T_{m,n}^{j}\right)$$

$$\left.+\left(\frac{k_{(m+1),(n+1)}^{j} + k_{m,n}^{j}}{2}\right)\left(T_{(m+1),(n+1)}^{j} - T_{m,n}^{j}\right)\right\}. \qquad (3)$$

Auxiliary equations

To calculate the temperatures of the elements along the lines of symmetry A-C and B-C, the temperature has to satisfy the following symmetry conditions:

line A–C

$$T_{M,1}^{j+1} = T_{M,3}^{j+1} \tag{4}$$

line B–C

$$T_{m,(N-m)}^{j+1} = T_{(m+1),(N-m+1)}^{j+1}. \tag{5}$$

In order to ensure that any error existing in the solution at some time level will not be amplified in subsequent calculations, a stability criterion has to be satisfied which, for a selected value of $\Delta\xi$, limits the maximum of the time step ($\Delta\tau$). Following the method described in reference [11], it can be derived that for the fire-exposed column the criterion of stability is most restrictive along the line m+1, between fire and concrete. It is given by the condition:

$$\Delta\tau \leq \frac{(\Delta\xi)^2}{\dfrac{4k_{max} + 2\sqrt{Z}\,\Delta\xi\, h_{max}}{(\rho_c c_c)_{min}}} \tag{6}$$

where the maximum value of the coefficient of heat transfer during exposure to the standard fire (h_{max}) is approximately 3×10^6 J/m^{2}h°C (147 Btu/ft^{2}h°F).

Effect of moisture

The effect of moisture is taken into account by assuming that in each element, the moisture starts to evaporate when the temperature of the element reaches 100°C (212°F). During the period of evaporation all the heat supplied to an element is used for evaporation of the moisture, until the element is dry. From a heat balance equation, the moisture concentration in an element at the fire/concrete boundary, at the time $\tau = (j+1)\Delta\tau$ is given by:

$$\phi_{1,n}^{j+1} = \phi_{1,n}^{j} - \frac{2\Delta\tau}{\rho_w \lambda_w (\Delta\xi)^2}\left\{\left(\frac{k_{2,(n-1)}^{j} + k_{1,n}^{j}}{2}\right)\left(T_{2,(n-1)}^{j} - T_{1,n}^{j}\right)\right.$$
$$+\left(\frac{k_{2,(n+1)}^{j} + k_{1,n}^{j}}{2}\right)\left(T_{2,(n+1)}^{j} - T_{1,n}^{j}\right)$$
$$\left. + \sqrt{Z}\,\Delta\xi\sigma\varepsilon_f\varepsilon_c\left[(T_f^j + 273)^4 - (T_{1,n}^j + 273)^4\right]\right\}. \tag{7}$$

Similarly, the moisture concentration in an element inside the concrete at the time $\tau = (j+1)\Delta\tau$ is given by:

$$\phi^{j+1}_{m,n} = \phi^{j}_{m,n} - \frac{\Delta\tau}{\rho_w \lambda_w (\Delta\xi)^2} \left\{ \left(\frac{k^j_{(m-1),(n-1)} + k^j_{m,n}}{2} \right) \left(T^j_{(m-1),(n-1)} - T^j_{m,n} \right) \right.$$
$$+ \left(\frac{k^j_{(m+1),(n-1)} + k^j_{m,n}}{2} \right) \left(T^j_{(m+1),(n+1)} - T^j_{m,n} \right)$$
$$+ \left(\frac{k^j_{(m-1),(n+1)} + k^j_{m,n}}{2} \right) \left(T^j_{(m-1),(n+1)} - T^j_{m,n} \right)$$
$$\left. + \left(\frac{k^j_{(m+1),(n+1)} + k^j_{m,n}}{2} \right) \left(T^j_{(m+1),(n+1)} - T^j_{m,n} \right) \right\}. \qquad (8)$$

With the aid of equations (1) to (8), and the relevant material properties given in Appendix A, the temperature distribution in the column and on its surface can be calculated for any time ($\tau = (j+1)\Delta\tau$) if the temperature distribution at the time $j\Delta\tau$ is known. Starting from a temperature of 20°C (68°F), the temperature history of the column can be calculated by repeated application of equations (1) to (8).

Calculation of Strength during Fire

Transformation into square network

To simplify the calculation of the deformations and stresses in the column, the triangular network is transformed into a square network. In Fig. 10 a quarter section of this network, consisting of square elements arranged parallel to the x- and z-axis of the section, are shown. The width of each element of this network is $\Delta\xi/\sqrt{2}$. The temperatures, deformations and stresses of each element are represented by those of the center of the element. The temperature at the center of each element is obtained by averaging the temperatures of the elements in the triangular network according to the relation:

$$\left(T^j_{m,n} \right)_{\text{square}} = \left(\frac{T^j_{(m+1),(n+1)} + T^j_{m,(n+2)}}{2} \right)_{\text{triangular}} \qquad (9)$$

where the subscripts 'square' and 'triangular' refer to the elements of the square and triangular network.

During exposure to fire the strength of the column decreases with the duration of exposure. The strength of the column can be calculated by a method based on load-deflection analysis which in turn is based on a stress-strain analysis of cross-sections [2]. In this method, the columns, which are fixed at the ends during the tests, are idealized as pin-ended columns of reduced length KL (Fig. 11). The load on the test columns is intended to be concentric. To represent imperfections in the columns, an initial deflection y_o = 2.5 mm (0.1 in.) is assumed.

The curvature of the column is assumed to vary from zero at pin-end to mid-height according to a straight line relation, as illustrated in Fig. 11. For such a relation the deflection at mid-height (y), in terms of the curvature (χ) of the column at this height, can be given by:

$$y = \chi \frac{(KL)^2}{12} . \qquad (10)$$

For any given curvature (χ), and thus for any given deflection at mid-height, the axial strain is varied until the internal moment at the midsection is in equilibrium with the applied moment given by the product of load and total deflection. In this way a load deflection curve can be calculated for specific times during the exposure to fire. From these curves the strength of the column (its maximum load carrying capacity) can be determined for each time. In the calculation of column strength the following assumptions were made.

1) The properties of the concrete and steel are as given in Appendix A and later in this section.
2) The influence of the presence of reinforcing steel on the temperature may be neglected. Thus the column, from a thermal point of view, may be treated as consisting entirely of concrete. The temperature of the steel is assumed to be equal to the temperature in the column section at the location of the center of the steel.
3) Concrete has no tensile strength.
4) Plane sections remain plane.
5) Initial strains in the column before the exposure to fire consists of free shrinkage of the concrete and creep. Because mortar was inserted at the top to make good contact between the concrete and the steel end plate, the initial shrinkage will be assumed to be negligible.

The tests of the columns were started after a preloading period of about one hour. The shortening of the column due to creep in this period is assumed to be negligible.

Based on these assumptions, the change of column strength during the exposure to fire was calculated. In the calculations the square network shown in Fig. 10 was used. Because the strains and stresses of the elements are not symmetrical with respect to the x-axis, the calculations of the strains and stresses were performed for both the network shown and an identical network at the left of the x-axis. The force and moment in the section were obtained by adding the forces carried by each element and the moments contributed by them.

The equations used in the calculations of the strength of the column during the exposure to fire are given below.

Equations for the steel

From the assumption that plane sections remain plane, the strain in the reinforcing steel is equal to the axial strain of the column (ε) and the

strain due to bending of the column (z_s/ρ), where z_s is the horizontal distance of the reinforcing steel bar to the vertical plane through the x-axis of the section of the column, and ρ is the radius of curvature. The strain causing stress, however, is determined as the difference between this strain and the free strain $[(\varepsilon_T)_s]$ that would take place due to thermal expansion of the steel. For the steel at the right of the x-axis, this strain $[(\varepsilon_s)_R]$ is given by:

$$(\varepsilon_s)_R = -(\varepsilon_T)_s + \varepsilon + \frac{z_s}{\rho} . \tag{11}$$

For the steel elements at the left of the x-axis, the strain $[(\varepsilon_s)_L]$ is given by:

$$(\varepsilon_s)_L = -(\varepsilon_T)_s + \varepsilon - \frac{z_s}{\rho} . \tag{12}$$

The stresses in the elements of the network are calculated using stress-strain relations derived from data provided by Ingberg and Sale [12], and Witteveen, Twilt and Bylaard [13]. These relations include the effect of creep at elevated temperatures and were obtained at heating rates approximately those that occur in a fire in actual practice. The relations have been generalized for other structural steels by assuming that, for a given temperature, the curves are the same for all steels, but the stress below which the stress-strain relation is linear, is proportional to the yield strength of the steel. This is illustrated in Fig. 12, where the stress-strain curves at 20°C (68°F) are shown for a steel with a yield strength of 250 MPa (36 psi) and for the reinforcing steel, which has a yield strength of 443 MPa (64.3 psi). In Fig. 13 the stress-strain curves of the reinforcing steel are shown for various temperatures. These curves reflect that even at the very high temperature of 800°C (1472°F) the steel still possesses some strength and rigidity. The equations that describe the relation between the stress in the steel (f_y), the strain (ε_s) and the temperature of the steel (T) are as follows:

for

$$\varepsilon_s < \varepsilon_p$$

$$f_y = \frac{f(T,0.001)}{0.001}\,\varepsilon_s \tag{13}$$

where

$$\varepsilon_p = 4 \times 10^{-6} f_{yo} \tag{14}$$

and

$$f(T,0.001) = (50-0.04T) \times \left[1-\exp\left((-30+0.03T)\sqrt{0.001}\right)\right] \times 6.9 \tag{15}$$

for

$$\varepsilon_s > \varepsilon_p$$

$$f_y = \frac{f(T,0.001)}{0.001}\varepsilon_p + f(T,(\varepsilon_s-\varepsilon_p+0.001)) - f(T,0.001)\,] \quad . \qquad (16)$$

With the aid of equations (10)-(16) the stresses at mid-height in the steel can be calculated for any value of the axial strain (ε), curvature ($1/\rho$) and temperature (T). From these stresses the load that the steel carries and the contribution of the steel to the moments can be derived.

Equations for the concrete

In the same way as for steel, the strain in the concrete causing stress for elements at the right of the x-axis (Fig. 10) can be given by:

$$(\varepsilon_c)_R = -(\varepsilon_T)_c + \varepsilon + \frac{z_c}{\rho} \qquad (17)$$

and for elements at the left of the x-axis by:

$$(\varepsilon_c)_L = -(\varepsilon_T)_c + \varepsilon - \frac{z_c}{\rho} \qquad (18)$$

where

$(\varepsilon_T)_c$ = free strain due to thermal expansion of the concrete,
ε = axial strain of the column,
z_c = horizontal distance of the center of the element to the vertical plane through the x-axis of the column section,
ρ = radius of curvature.

The stresses in the elements are calculated using stress-strain relations based on the work of Ritter [14] and Hognestad [15]. These relations have been slightly modified to take into account the creep of concrete at elevated temperatures. The modifications are based on results of work by Schneider and Haksever [16] and consist of a movement of the maxima in the stress-strain curves to higher strains with higher temperatures. These curves are shown in Fig. 14 for a concrete with a cylinder strength of 35 MPa (5 ksi). The equations that describe these curves are as follows:

for

$$\varepsilon_c \leq \varepsilon_{max}$$

$$f_c = f'_c \left[1 - \left(\frac{\varepsilon_{max} - \varepsilon_c}{\varepsilon_{max}}\right)^2\right] \qquad (19)$$

for

$$\varepsilon_c > \varepsilon_{max}$$

$$f_c = f'_c \left[1 - \left(\frac{\varepsilon_c - \varepsilon_{max}}{3\ \varepsilon_{max}}\right)^2\right] \qquad (20)$$

where

$$f'_c = f'_{co} \text{ if } T < 450°C \qquad (21)$$

$$f'_c = f'_{co} \left[2.011 - 2.353\ \frac{T-20}{1000}\right] \text{ if } T > 450°C \qquad (22)$$

$$\varepsilon_{max} = 0.0025 + (6.0T + 0.04T^2) \times 10^{-6}\ . \qquad (23)$$

In these equations

f_c = compressive strength of concrete at temperature T,
f'_c = cylinder strength of concrete at temperature T,
f'_{co} = cylinder strength of concrete at 20°C (68°F),
ε_c = strain of the concrete,
ε_{max} = strain corresponding to maximum stress.

With the aid of equations (17)-(23) the stresses in each of the concrete elements at midsection can be calculated for any value of the axial strain (ε) and curvature ($1/\rho$). From these stresses the load that the concrete carries and the contribution of the concrete to the moments can be derived.

TEST CONDITIONS AND PROCEDURE

The tests were carried out by exposing the columns to heat in a furnace specially built for this purpose. The heat input into the test furnace was controlled in such a way that the average temperature followed as closely as possible the standard temperature/time curve given by Eq. (1). The instrumentation and characteristics of the furnace are described in detail in reference [17]. The columns were attached by bolting t' end plates to a loading head at the top and a hydraulic jack at the bottom. For this purpose, eight 19 mm (3/4 in.) bolts, spaced regularly around the column 63.5 mm (2 1/2 in.) from the sides were used at each end.

Several of the columns were tested under a load, which was concentric. The loads were applied about one hour prior to the test.

On the date of testing, the relative humidity in the center of the concrete and the cylinder strength of the concrete were measured. The measured values are given in Table I.

During the test, measurements were made of furnace temperatures at eight locations with the aid of thermocouples. The junction of each thermocouple was located 305 mm (1 ft) from the test specimen, at various heights. Two thermocouples are placed opposite each other every 610 mm (2 ft) along the height of the furnace chamber. The location of their junctions and their numbering are shown in Fig. 15. Thermocouples No. 4 and 6 were located at a height of 610 mm from the floor, thermocouples No. 2 and 8 at 1220 mm (4 ft), thermocouples No. 3 and 5 at 1830 mm (6 ft) and thermocouples No. 1 and 7 at 2440 mm (8 ft).

Measurements were also made of the temperatures of the concrete and steel in the column at the locations described earlier. The axial strain of those columns that were tested under a load was also measured. These columns were considered to have failed, and the test was terminated, when the hydraulic jack, which has a maximum speed of 76 mm/min (3 in./min), could no longer maintain the applied load. Unloaded columns, which were tested to obtain information on the temperature history in the column, were exposed to fire for 3 to 5 hours, depending on their size. The duration of the various tests, and the loads that were applied, are given in Table VIII.

RESULTS* AND DISCUSSION

Furnace Temperatures

The first test was carried out to obtain information on the control and uniformity of temperatures in the furnace chamber. The temperatures in the furnace measured during this test at the various thermocouple locations and their average, as well as the standard fire temperatures according to ASTM E119 [8] or ULC S101 [9], are given as a function of time in Table IX. In the period of rapid temperature rise (to about ten minutes) there are relatively large differences between the temperatures measured at various heights and between the average furnace temperatures and standard fire temperatures. After that, these differences become small and a high temperature uniformity, as well as average furnace temperatures that follow closely the standard fire temperatures, were obtained.

Because the period of substantial temperature variability is short, the influence of this variability on temperatures in the column is not significant for fire exposure periods of interest (about one hour or more). The small influence of the initial variability of furnace temperature can be shown by comparing the temperatures measured at various heights at specific depths in the concrete.

Temperatures in Concrete

The temperatures measured in the concrete at various heights and depths are shown in Fig. 16 for columns No. 1, 5 and 6 in Table VIII. For specific depths, the differences in temperature between the various heights are small after an exposure time of about one hour. The small differences indicate

*Detailed information on test results is available from the first author.

that, for exposure periods of one hour or longer, the heat transfer from the furnace to the column may be regarded as uniform.

In Fig. 17 the average of the temperatures, measured in the same columns at one-quarter height, mid-height and three-quarter height, are shown for three depths in each column. Also shown are calculated temperatures for the corresponding depths. The calculations were carried out for dry concrete. Although the test columns were in near oven-dry condition at the time of testing, they still contained a small amount of moisture. There is a rapid rise of the temperatures measured in the deeper part of the concrete in the earlier stages of the tests. This rise may result from thermally-induced migration of moisture towards the center of the column. At a later stage, however, which is the important stage for predicting the fire resistance of the columns, there is good agreement between measured and calculated temperatures.

Temperatures of Steel

The temperatures measured on the main reinforcing steel bars are shown in Fig. 18 for columns No. 1, 5 and 6 in Table VIII. These measurements were made in column No. 6 with thermocouples No. 3 and 9, located opposite each other with respect to the center of one bar, and with thermocouples No. 4 and 8, located opposite each other on another bar (Fig. 6). The measurements in column No. 1 were made with thermocouples No. 3 and 9, located opposite each other on one bar, and thermocouples No. 4 and 10, located in similar positions on another bar (Fig. 7). The measurements in column No. 5 were made with thermocouples No. 6 and 11 on one bar and No. 4 and 12 on another bar (Fig. 8). The curves in Fig. 18 show that the differences in temperature between two opposite points of the bar are relatively small. Therefore, the average of the temperatures measured at opposite locations on a bar is a good approximation of the average steel temperature.

In Fig. 19 the average steel temperature is compared with temperatures calculated as described earlier in this paper. In this method, the column is treated as consisting entirely of concrete, and the temperature at the location of the center of the steel is chosen as representative of the average temperature of the steel. Calculated steel temperatures are somewhat higher than measured steel temperatures. The differences are small, however. Because at high temperatures the steel is contributing only a relatively small part to the strength of the column, small deviations in steel temperature have little influence on the column strength. The method is therefore sufficiently accurate for calculating steel temperatures.

Influence of Load

To study the influence of load on fire resistance, five identical columns, made with siliceous aggregate, were tested under different loads. The columns tested, which had a section size of 305 mm (12 in.) square, were specimens No. 3, 4, 7, [illegible]nd 9 in Table VIII. During the tests concentric loads of 800, 711, 1067, 1778 and 1333 kN (180, 160, 240, 400 and 300 kips) respectively, were applied.

Calculations were also made of the fire resistance of these columns as a function of the load. It was assumed that the moisture content in the concrete was 5% by volume and the concrete strength was 35 MPa (5 ksi).

How the load affects the fire resistance of the columns is shown in Fig. 20, where measured and calculated fire resistances for various loads are given. Both measured and calculated results show a strong influence of the load on the fire resistance of the columns. Calculated fire resistances, however, are somewhat lower than measured fire resistances. The differences range from about 2 to 16% of the measured fire resistances.

The maximum allowable load for these columns, for an effective column length of 3810 mm (12 ft 6 in.), is about 900 kN (200 kips), according to ACI 318 [6] or CSA A23 [7]. For this load, the fire resistance of the column is more than 3 hours. At present the National Building Code of Canada [18] and ACI Guide 216 [19] assign a fire resistance of about 2 hours to this column.

Part of the procedure of calculation of fire resistance is the calculation of the axial deformation of the columns. This deformation was also measured during the tests on loaded columns. Typical curves for measured and calculated axial deformations are shown in Figs. 21 and 22. In Fig. 21 the axial deformation is shown as a function of time for column No. 3 (Table VIII), which was tested under a load of 800 kN (180 kips) and in Fig. 22, for column No. 7, tested under a load of 1067 kN (240 kips). In all cases where the axial deformation was measured, there was relatively good agreement between the theoretical and the experimentally derived curves. Near the failure point, however, measured contractions of the column are greater than those calculated. A possible reason for the difference is that the concrete is more ductile at high temperature than assumed in the model. The influence of this difference on the fire resistance is about ten minutes. It is small in comparison with the fire resistance of the column, but can eventually be taken into account empirically.

Influence of Cross-Section

In this phase the influence of cross-section was studied mainly from a thermal point of view. All columns tested under a load had a section size of 305 × 305 mm (12 × 12 in.), except one, which had a section size of 203 × 203 mm (8 × 8 in.). All columns failed in compression except the smaller one, which failed by buckling.

The influence of section size on the temperatures in the concrete can be derived from the temperature curves given in Fig. 17. For example, it takes about 60 minutes to reach a temperature of 300°C at mid-depth in the 203 × 203 mm column section, 90 minutes in the 305 × 305 mm section and 180 min in the 406 × 406 mm section. The influence of section size on fire resistance, for a specific load, will be even greater than the influence on temperature because, in addition to the slower temperature rise, the larger column also has more area of low temperature that can contribute to carrying the load.

Influence of Moisture

The influence of moisture on fire resistance was studied theoretically as well as experimentally. For this purpose a column (No. 2, Table VIII) was tested in a nearly dry state under a load equal to that on a similar, but normally-conditioned, test column (No. 9). Calculations were also made of the temperatures in the column during fire exposure and of its fire resistance as a function of load.

In Fig. 23 measured temperatures, and in Fig. 24 calculated temperatures, at various depths in the column, are given as a function of time. The maximum delay in temperature rise, at 180 minutes, due to moisture, is about 20 minutes according to the measurements and about 15 minutes according to the calculations.

The influence of moisture on the fire resistance of the column is shown in Fig. 25. In this figure, calculated fire resistances are given as a function of load for a dry column and for a column with a moisture content of 5% by volume, representing a normal moisture condition. For a load of 1333 kN (300 kips), the load on the columns during the tests, the calculated influence of moisture on fire resistance is about ten minutes. Somewhat higher fire resistances were obtained in the tests than those calculated. Also a somewhat higher influence of moisture on fire resistance (17 minutes) was found.

The results of tests and calculations indicate that for normal fluctuations in the moisture condition of the concrete (for example, a moisture content of 3 to 5%), moisture has only a small effect on the fire resistance of the column.

Influence of Aggregate

Three columns made with carbonate aggregate were tested under different loads (columns No. 10, 11 and 12 in Table VIII). A comparison with the fire resistance of similar columns, made with siliceous aggregate and tested under the same loads, showed that the fire resistance of the carbonate aggregate columns was much higher than that of the siliceous aggregate columns. Under approximately the maximum allowable load, the fire resistance of the carbonate aggregate column (No. 11) was almost twice as high as that of the siliceous aggregate column (No. 7). The difference was partly caused by a slower temperature rise in the carbonate aggregate column, particularly at higher temperatures (Fig. 26). A substantial part of the difference was due to the high ductility of the carbonate aggregate concrete, which enables the column to undergo large axial deformations without failure (Fig. 27).

No calculations were made of the fire resistance of the carbonate aggregate columns because the material properties of the concrete of which the columns were made, were not sufficiently known. Further studies are needed to determine the thermal and mechanical properties of this concrete at elevated temperatures.

CONCLUSIONS

Of the variables studied in the first phase of the study program, load, cross-section size and type of aggregate have the largest influence on the fire resistance of reinforced concrete columns. Particularly the use of carbonate aggregate instead of siliceous aggregate will substantially increase the fire resistance of the column. The influence of concrete moisture content on fire resistance is, in the practical range, insignificant.

The fire resistances of the columns studied are considerably higher than those assigned to them in the National Building Code and in the American Concrete Institute Guide 216.

Column temperatures, deformations and fire resistances calculated using the mathematical model described in the present paper are in good agreement with those measured.

The experimental results provide basic data on the fire resistance of columns under standard fire test conditions. They also enable the evaluation of assumptions used for calculating fire resistance by methods based on heat transfer and structural analyses.

To develop general methods for the determination of the fire resistance of concrete columns and walls for a wide range of applications, a second phase of studies is planned. In this phase the effect of the following on fire resistance will be studied:

1) restraint of column expansion,
2) strength of concrete,
3) use of lightweight aggregate,
4) amount of steel,
5) thickness of concrete cover to steel.

References

1. Lie, T.T. and Allen, D.E. (1972). Calculations of the Fire Resistance of Reinforced Concrete Columns, National Research Council of Canada, Division of Building Research, NRCC 12797, Ottawa.

2. Allen, D.E. and Lie, T.T. (1974). Further Studies of the Fire Resistance of Reinforced Concrete Columns, National Research Council of Canada, Division of Building Research, NRCC 14047, Ottawa.

3. Standard Practice for Petrographic Examination of Aggregates for Concrete, (1979). ASTM C295-79, American Society for Testing and Materials, Philadelphia.

4. Standard Specification for Deformed and Plain Bullet-Steel Bars for Concrete Reinforcement, (1980). ASTM A615-80, American Society for Testing and Materials, Philadelphia.

5. Reinforcing Steel Welding Code, (1975). AWS-D12.1-75, American Welding Society, Manlius, N.Y.

6. Building Code Requirements for Reinforced Concrete, (1977). ACI Standard 318-77, American Concrete Institute, Detroit.

7. Code for the Design of Concrete Structures for Buildings, (1977). CAN3-A23.3-M77, Canadian Standards Association, Rexdale, Ontario.

8. Standard Methods of Fire Tests of Building Construction and Materials, (1979). ANSI/ASTM E119-79, American Society for Testing and Materials, Philadelphia.

9. Standard Methods of Fire Endurance Tests of Building Construction and Materials, (1980). ULC-S101-M1980, Underwriters' Laboratories of Canada, Scarborough, Ontario.

10. Lie, T.T. and Harmathy, T.Z. (1972). A Numerical Procedure to Calculate the Temperature of Protected Steel Columns Exposed to Fire, Fire Study No. 28, Division of Building Research, National Research Council of Canada, NRCC 12535, Ottawa.

11. Dusinberre, G.M. (1961). Heat Transfer Calculations by Finite Differences, International Textbook Company, Scranton, Pa.

12. Ingberg, S.H. and Sale, P.D. (1926). Compressive Strength and Deformation of Structural Steel and Cast-Iron Shapes at Temperatures up to 950°C (1742°F). Proceedings of the American Society for Testing and Materials, Vol. 26, II, Philadelphia.

13. Witteveen, J., Twilt, L. and Bylaard, F.S.K. (1977). The Stability of Braced and Unbraced Frames at Elevated Temperatures, Second Int. Colloquium on Column Strength, Liege, April 1977.

14. Ritter, W. (1899). Die Bauweise Hennebique, Schweizerische Bauzeitung, Vol. 33, February.

15. Hognestad, E. (1951). A Study of Combined Bending and Axial Load in Reinforced Concrete Members, University of Illinois Engineering Experiment Station Bulletin No. 399, Urbana.

16. Schneider, U. and Haksever, A. (1976). Bestimmung der aquivalenten Branddauer von statisch bestimmt gelagerten Stahlbetonbalken bei naturlichen Branden, Bericht des Instituts fur Baustoffkunde und Stahlbetonbau der Technischen Universitat Braunschweig.

17. Lie, T.T. (1980). New Facility to Determine Fire Resistance of Columns, Canadian Journal of Civil Engineering, Vol. 7, No. 3.

18. The Supplement to the National Building Code of Canada, (1980). Associate Committee on the National Building Code, National Research Council of Canada, NRCC No. 17724, Ottawa.

19. Guide for Determining the Fire Endurance of Concrete Elements, (1981). Concrete International, Report No. ACI 216R-81, Detroit.

20. Harmathy, T.Z. and Allen, L.W. (1973). Thermal Properties of Selected Masonry Unit Concretes, Journal of the American Concrete Institute, Vol. 70.

TABLE I. DETAILS CONCERNING 1ST PHASE COLUMN TEST SPECIMENS
(cross sections 305 × 305 mm (12 × 12 in.) unless otherwise noted)

Specimen no.	Cast date	Test date	Moisture condition of specimen at test date (% RH)	Compressive strength of cylinders at 28 days MPa (psi)	Compressive strength of cylinders at test date[c] MPa (psi)
Siliceous aggregate					
1	77-6 -27	79-9 -19	5	34.2 (4953)	not measured
2	77-7 -7	81-6 -19	15	31.0 (4502)	37.3 (5402) 36.6 (5305)
3	77-7 -14	80-4 -25	70	34.8 (5046)	34.2 (4961) 34.2 (4952)
4	77-7 -20	80-3 -19	63	31.7 (4603)	35.9 (5199) 34.5 (4996) 35.8 (5190)
5[a]	77-7 -29	81-1 -23	9	35.7 (5170)	42.6 (6172) 38.8 (5633)
6[b]	77-7 -26	82-3 -12	29	34.8 (5040)	42.6 (6172) 42.1 (6109)
7	77-8 -1	80-7 -11	74	35.3 (5117)	36.8 (5332) 35.4 (5129)
8	77-8 -5	80-9 -12	74	33.5 (4863)	34.2 (4952) 35.4 (5138)
9	77-8 -19	81-2 -5	75	36.8 (5330)	39.7 (5757) 37.0 (5359)
Carbonate aggregate					
10	77-8 -19	81-12 -14	75	33.6 (4875)	40.9 (5925)
11	77-8 -25	81-10 -13	75	33.5 (4860)	37.1 (5386) 36.7 (5315)
12	77-8 -30	82-1 -22	76	34.2 (4960)	38.5 (5580) 41.4 (5996)

[a]cross section 406 × 406 mm (16 × 16 in.)
[b]cross section 203 × 203 mm (8 × 8 in.)
[c]results of one or more cylinder tests are given

TABLE II. PETROGRAPHY OF SAND AND GRAVEL USED AS SILICEOUS AGGREGATE

Component	Composition of Sieve Fraction, Percent on Sieve of Size Indicated											Percent Passing through No. 200
	19 mm	12.5 mm	9.5 mm	6 mm	No. 4	No. 8	No. 16	No. 30	No. 50	No. 100	No. 200	
Granite	37.9	32.9	25.5	31.3	27.0	27.6	12.3	7.4	1.9	4.4	0.6	—
Quartzite	21.6	29.2	34.8	24.6	24.5	20.0	12.3	12.6	10.9	3.1	2.2	—
Quartz	6.3	3.1	4.9	4.8	5.5	18.8	52.2	62.0	73.1	79.5	74.2	92.0
Chert[a]	10.8	7.0	5.2	8.1	9.8	5.9	7.7	3.5	2.0	0.8	2.8	2.0
Sandstone-Quartz Conglomerate	1.9	0.8	3.1	5.1	5.5	8.3	—	—	—	—	—	—
Rhyolite-Dacite	13.9	6.2	2.2	5.1	7.2	4.1	0.8	2.6	1.6	0.8	0.9	—
Feldspar	—	—	—	—	—	—	1.3	5.0	6.6	5.0	10.8	4.0
Diorite	1.9	1.4	3.1	1.8	1.2	—	—	—	—	—	—	—
Graywacke[b]	1.3	9.5	5.8	5.4	4.3	6.5	2.3	1.5	0.3	—	0.6	—
Gneiss-Schist	2.5	5.1	10.5	9.3	7.5	4.1	6.4	1.8	0.9	1.1	0.6	—
Basalt	1.9	4.5	4.0	3.9	6.9	3.2	2.6	2.4	0.7	—	0.3	—
Misc. Igneous Rocks and Opaque Minerals	—	0.3	0.9	0.6	0.6	1.5	2.1	1.2	2.0	5.3	7.0	2.0

Particle Shape	19 to 6 mm (%)	No. 4 to No. 16 (%)	No. 30 to No. 200 (%)
Subrounded to rounded	30	20	10
Subrounded to subangular	40	40	40
Angular	30	40	50

[a] "Ironstone," made up of jasper and hematite, is included in the chert classification.
[b] Includes metagraywacke.
[c] The miscellaneous igneous rocks were severely altered and positive identification was impossible. The opaque minerals occurred in the No. 50 and smaller sieve sizes and were largely magnetite.

TABLE III. PETROGRAPHY OF SAND AND GRAVEL USED AS CARBONATE AGGREGATE

Component	Composition of Sieve Fraction, Percent on Sieve of Size Indicated											Percent passing through No. 200
	19 mm	12.5 mm	9.5 mm	6 mm	No. 4	No. 8	No. 16	No. 30	No. 50	No. 100	No. 200	
Carbonate	91.1	87.4	87.3	85.6	87.6	80.5	79.6	64.4	46.1	36.4	65.0	92.0
Chert	3.6	4.2	5.2	7.6	6.1	8.9	11.0	--	--	--	--	--
Granite	1.1	1.2	3.5	1.8	2.4	3.6	2.4	--	--	--	--	--
Basalt	2.1	3.0	1.4	2.6	2.6	3.4	2.0	1.2	--	--	--	--
Gabbro	0.3	--	--	0.2	0.5	0.2	0.7	0.3	--	--	--	--
Quartzite	1.8	3.9	1.4	1.3	0.3	3.0	4.3	--	--	--	--	--
Gneiss-Schist	--	0.3	1.2	0.9	0.5	0.4	--	--	--	--	--	--
Quartz-Chalcedony	--	--	--	--	--	--	--	26.5	45.1	52.5	27.2	4.0
Feldspar	--	--	--	--	--	--	--	7.6	8.8	11.1	6.1	0.5
Misc. Igneous and Clays	--	--	--	--	--	--	--	--	--	--	1.7	3.5

Particle Shape	19 to 6 mm (%)		No. 4 to No. 200 (%)	
	Carbonates	Silicates	Carbonates	Silicates
Rounded	--	--	--	30
Subangular to subrounded	80	100	75	60
Angular	--	--	--	10
Angular to subangular	20	--	25	--

TABLE IV. PHYSICAL PROPERTIES OF AGGREGATES

	Siliceous	Carbonate
Specific gravity of sand	2.63	2.67
Specific gravity of gravel	2.57	2.67
Moisture content of sand (%)	4.0	3.0
Moisture content of gravel (%)	1.0	1.0
Saturated surface dry density of gravel kg/m^3 (lb/ft^3)	1678 (104.9)	1712 (107.0)
Fineness modulus of fine aggregate	2.96	3.00
Fineness modulus of coarse aggregate	1.73	1.53

TABLE V. TENSILE STRENGTH OF STEEL

Bar size	Yield stress MPa	(psi)	Ultimate strength MPa	(psi)
10M	426.5	(61 818)	671.2	(97 272)
20M	442.2	(64 090)	721.4	(104 545)
25M	443.7	(64 303)	730.2	(105 822)

TABLE VI. BATCH QUANTITIES AND PROPERTIES OF CONCRETE

	With carbonate aggregate		With siliceous aggregate	
	kg/m^3	(lb/yd^3)	kg/m^3	(lb/yd^3)
Cement	345.9	(583)	307.3	(518)
Coarse aggregate	1065.5	(1796)	1054.3	(1777)
Sand	815.8	(1375)	871.5	(1469)
Water	192.8	(325)	153.7	(259)
Average air content (%)	1.9		1.7	
Average unit weight, kg/m^3 (lb/ft^3)	2403	(150)	2403	(150)
Average compressive strength at 28 days, MPa (psi)	33.8	(4898)	34.2	(4958)
Average slump, mm (in.)	76.2	(3.0)	83.82	(3.3)

TABLE VII. CONDITIONS CONSIDERED IN THE FIRST PHASE OF STUDY

Factor	Design according to CSA-CAN A23.3-M77 or ACI 318-77	Standard fire test	Assumed in mathematical model	Actual practice during fire
Load	All loads (dead, live, wind, earthquake) taken into account	Maximum allowable load determined according to ACI or CSA standards, or less, based on loads likely to occur during fire	Any load, greater than, equal to or less than the maximum allowable	Maximum load expected during fire. Only dead and sustained components of live loads are likely to be present
Column length	Height of column. In this case: ≈ 3.8 m (12.5 ft)	Not less than 2.7 m (9 ft); in this case: ≈ 3.8 m (12.5 ft)	Heated length + half of thicknesses of floor and roof insulation. In this case: ≈ 3.5 m (11 ft 4 in.)	Height of column
Effective length factor	K=1 if braced against side-sway (unless analysis shows that a lower value may be used)	Conditions assumed the same as in design. In this case: K=1; effective length of standard test specimen ≈ 3.8 m (12.5 ft)	K=0.6 if fixed at top and bottom. Thus effective column length is 0.6 × 3.45 m (11 ft 4 in.) = 2.07 m (≈ 6.8 ft)	≈ 0.6 during fire
Eccentricity	Minimum equal to the greater of 25 mm or 0.1 h (CSA) or (0.6 + 0.03 h) in. (ACI)	Concentric	Estimated at 2.5 mm (≈ 0.1 in.) for a test column	Varies with loading and end conditions; can be approximated by minimum eccentricity according to ACI or CSA

TABLE VII (Cont.)

Factor	Design according to CSA-CAN A23.3-M77 or ACI 318-77	Standard fire test	Assumed in mathematical model	Actual practice during fire
Strength of concrete	$0.85\ f'_c$ [f'_c = 35 MPa (5000 psi) unless it deviates by more than 10%]	$0.85\ f'_c$ [f'_c = 35 MPa (5000 psi) unless it deviates by more than 10%]	Given by Ritter's parabola with maximum stress f_c at room temperature, where f_c is average strength of two cylinders taken at time of test	Varies but for room temperature can be assumed equal to $0.85\ f'_c$ where f'_c is specified compressive strength of concrete (28 days cylinder strength)
Modulus of elasticity of concrete	$E_c = 50000\ \sqrt{f'_c}$ MPa(CSA) $E_c = 57000\ \sqrt{f'_c}$ psi(ACI) at room temperature	$E_c = 50000\ \sqrt{f'_c}$ MPa(CSA) $E_c = 57000\ \sqrt{f'_c}$ psi(ACI) at room temperature	Given by slope of stress-strain curve (Ritter's parabola) at variable temperatures	Varies but for room temperature can be assumed equal to design according to ACI or CSA
Strength of steel	f_y = 415 MPa (≃ 60000 psi) at room temperature	f_y = 415 MPa (≃ 60000 psi) at room temperature	Given by stress-strain curves for the the steel [f_y = 445 MPa (≃ 64300 psi) at room temperature]	Varies but for room temperature can be assumed f_y = 415 MPa (≃ 60000 psi)
Modulus of elasticity of steel	E_s = 200 000 MPa (29×10^6 psi) at room temperature	E_s = 200 000 MPa (29×10^6 psi) at room temperature	E_s given by slope of stress-strain curve for the steel [E_s = 200 000 MPa (29×10^6 psi) at room temperature]	E_s = 200 000 MPa (29×10^6 psi) at room temperature
Fire temperature/ time relation	NA	ASTM E119 or ULC-S101	ASTM E119 or ULC-S101	Any temperature/time relation, including decay period of fire

TABLE VIII. LOAD AND PERFORMANCE OF TEST COLUMNS
(cross-section 305 × 305 mm (12 × 12 in.) unless otherwise indicated)

Specimen no.	Load kN	Load (kips)	Length of test hr:min	Mode of failure
Siliceous aggregate				
1	0		4:00	None
2	1333	(300)	2:50	Compression
3	800	(180)	3:38	"
4	711	(160)	3:40	"
5[a]	0		5:00	None
6[b]	169	(38)	3:00	Buckling
7	1067	(240)	3:28	Compression
8	1778	(400)	2.26	"
9	1333	(300)	3:07	"
Carbonate aggregate				
10	800	(180)	8:30	"
11	1067	(240)	6:06	"
12	1778	(400)	3:36	"

[a]cross section 406 × 406 mm (16 × 16 in.)
[b]cross section 203 × 203 mm (8 × 8 in.)

TABLE IX. FURNACE TEMPERATURES (°C)

Time (min)	Measured at Thermocouple No: 1	2	3	4	5	6	7	8	Average Temperature	Standard Temperature
0	24	24	24	24	24	24	24	24	24	20
5	357	343	352	324	385	363	413	452	373	538
10	668	668	688	685	638	621	657	654	660	704
15	766	774	774	771	729	732	752	752	756	760
20	796	802	802	799	760	766	782	782	786	795
25	835	843	841	838	804	807	827	827	828	821
30	849	854	852	849	818	821	835	835	839	843
35	871	885	882	877	846	849	863	863	867	862
40	882	891	891	885	857	860	871	874	875	878
45	904	916	907	907	879	882	893	896	895	892
50	913	924	916	913	891	893	902	904	906	905
55	927	941	935	927	904	907	918	918	922	916
60	935	943	938	935	913	913	924	927	929	927
65	943	960	949	949	927	927	941	941	943	937
70	949	966	954	954	929	932	941	943	946	946
75	960	974	966	963	941	943	954	954	960	955
80	968	982	977	973	954	954	966	966	968	963
85	974	985	979	977	960	960	971	982	974	971
90	982	996	985	982	966	968	974	974	982	978
95	985	999	991	988	968	971	979	979	982	985
100	988	1004	993	993	974	977	982	985	988	991
105	996	1007	999	996	977	979	988	991	993	996
110	999	1010	1004	1002	982	982	993	996	999	1001
115	1002	1013	1004	1002	988	991	996	996	1002	1006
120	1004	1018	1010	1007	991	993	1002	1004	1007	1010
130	1013	1027	1018	1016	1002	1002	1010	1010	1016	1017
140	1018	1032	1024	1018	1004	1004	1010	1016	1018	1024
150	1024	1038	1027	1024	1010	1010	1018	1021	1024	1031
160	1029	1043	1032	1029	1018	1018	1024	1024	1027	1038
170	1029	1046	1038	1032	1021	1021	1027	1039	1032	1045
180	1038	1052	1043	1038	1027	1027	1033	1033	1038	1052

APPENDIX A

Material Properties and Physical Constants

The values of the material properties and physical constants used in this study are given below. With the exception of those for the thermal conductivity of concrete, the values are approximately those used in previous studies on reinforced concrete columns [1,2]. For the thermal conductivity, the values assumed to be valid for concrete made with pure quartz aggregate, were replaced by the values obtained by Harmathy and Allen [20] from tests on concrete with predominantly siliceous aggregate. Instead of tabulated values, approximate equations are used in this study to describe the relationship between the properties and temperature.

Concrete Properties

Thermal capacity of concrete

for $0 \leq T \leq 200°C$

$$\rho_c c_c = (0.005T + 1.7) \times 10^6 \quad J/m^3°C$$

for $200°C < T \leq 400°C$

$$\rho_c c_c = 2.7 \times 10^6 \quad J/m^3°C$$

for $400°C < T \leq 500°C$

$$\rho_c c_c = (0.013T - 2.5) \times 10^6 \quad J/m^3°C$$

for $500°C < T \leq 600°C$

$$\rho_c c_c = (-0.013T + 10.5) \times 10^6 \quad J/m^3°C$$

for $T > 600°C$

$$\rho_c c_c = 2.7 \times 10^6 \quad J/m^3°C$$

Thermal conductivity of concrete

for $0 \leq T \leq 800°C$

$$k = -0.000625T + 1.5 \quad W/m°C$$

for $T > 800°C$

$$k = 1.0 \quad W/m°C$$

Coefficient of thermal expansion

$$\alpha_c = (0.008T + 6) \times 10^{-6}$$

Steel Properties

Coefficient of thermal expansion

for $T < 1000°C$

$$\alpha_s = (0.004T + 12) \times 10^{-6}$$

for $T > 1000°C$

$$\alpha_s = 16 \times 10^{-6}$$

Water Properties

Thermal capacity

$\rho_w c_w = 4.2 \times 10^{-6}$ $J/m^3{}^\circ C$

Heat of vaporization

$\lambda_w = 2.3 \times 10^6$ J/kg

Physical Constants

σ = Stefan-Boltzmann constant: 5.67×10^{-8} W/m K

ε_f = emissivity of fire: 1

ε_c = emissivity of concrete: 0.9

Nomenclature

Notations

c	specific heat (J/kg°C)
f_c	compressive strength of concrete at temperature T (MPa)
f'_c	cylinder strength of concrete at temperature T (MPa)
f'_{co}	cylinder strength of concrete at room temperature (MPa)
f_y	strength of steel at temperacure T (MPa)
f_{yo}	yield strength of steel at room temperature (MPa)
h	coefficient of heat transfer at fire exposed surface ($W/m^2°C$)
k	thermal conductivity (W/m°C)
K	effective length factor
L	unsupported length of column (m)
P	point
T	temperature (°C)
x	coordinate
y	lateral deflection of column at mid-height (m)
z	coordinate

Greek letters

α	coefficient of thermal expansion
Δ	increment
$\Delta\xi$	mesh width (m)
ε	emissivity, strain (m)
λ	heat of vaporization (J/kg)
ρ	density (kg/m^3), radius of curvature (m)
σ	Stefan-Boltzmann constant (W/m^2K^4)
τ	time (h)
ϕ	concentration of moisture (fraction of volume)
χ	curvature of column at mid-height (m^{-1})

Subscripts

o	at room temperature
c	of concrete
f	of the fire
m,M	at the points m, M in column
max	maximum
min	minimum
n,N	at the points n, N in a row
L	left of the x-axis
R	right of the x-axis
p	pertaining to proportional stress-strain relation
s	of steel
T	pertaining to temperature
w	of water

Superscripts

j	at $\tau = j\Delta\tau$

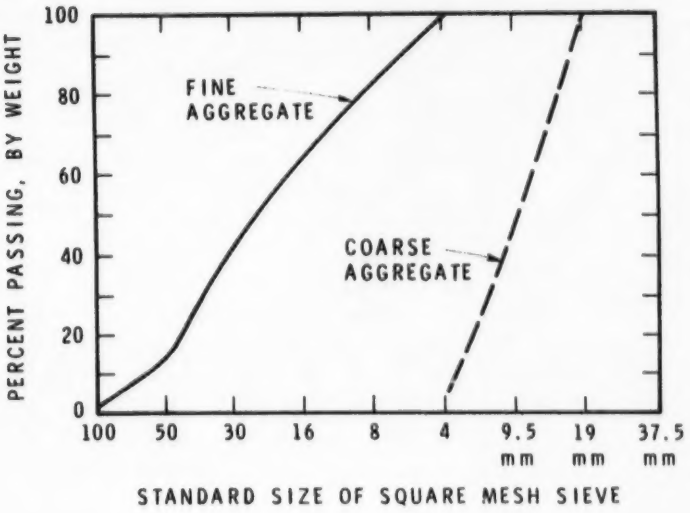

FIGURE 1
GRADATION CURVES OF CARBONATE AGGREGATE

BR 6444-1

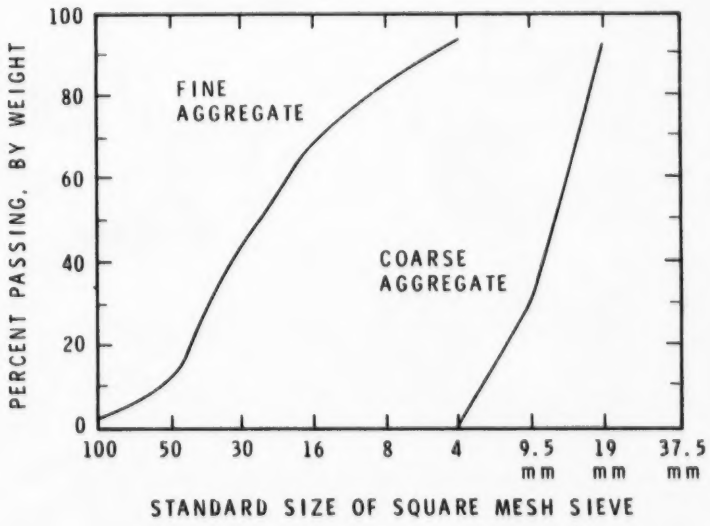

FIGURE 2
GRADATION CURVES OF SILICEOUS AGGREGATE

BR 6432-1

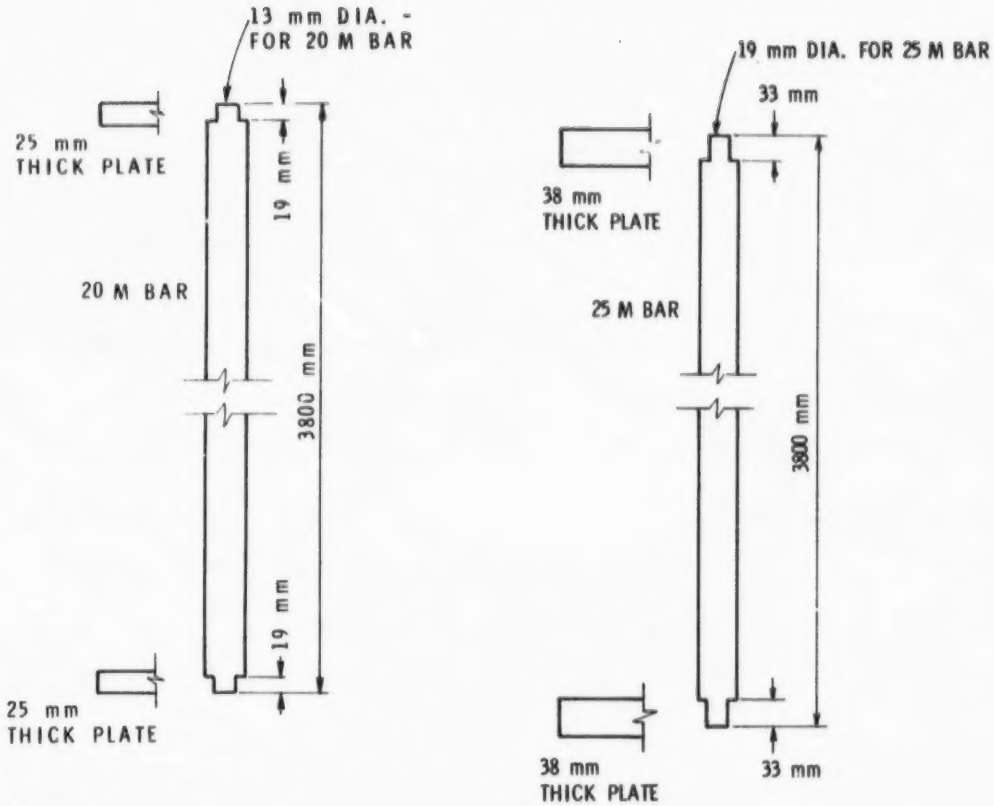

FIGURE 3

MAIN REINFORCING BARS

BR 6446-1

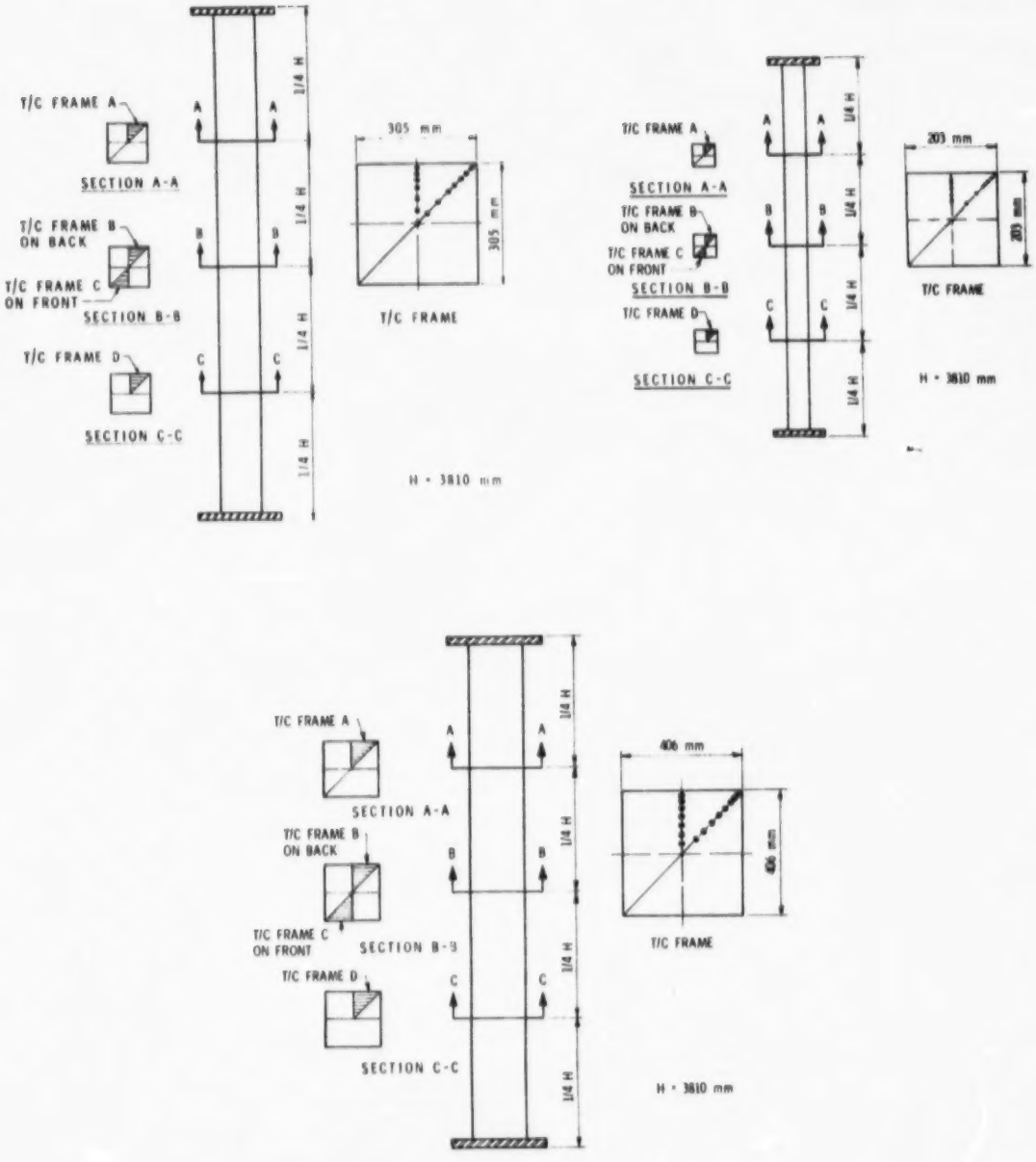

FIGURE 4
LAYOUT OF THERMOCOUPLE FRAMES

BR 6441-7

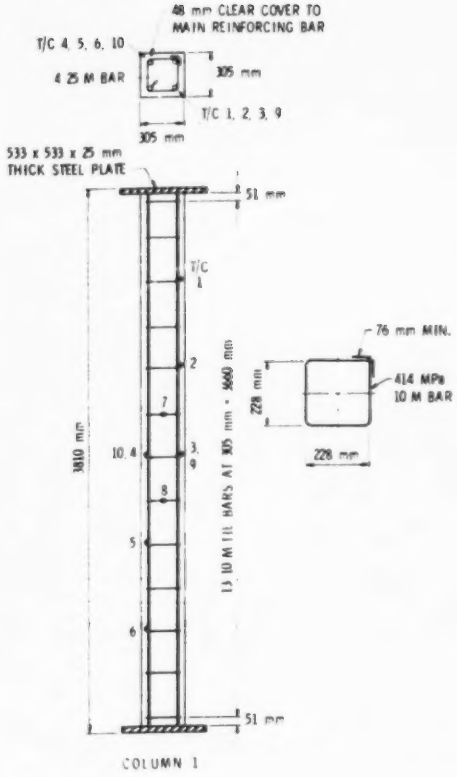

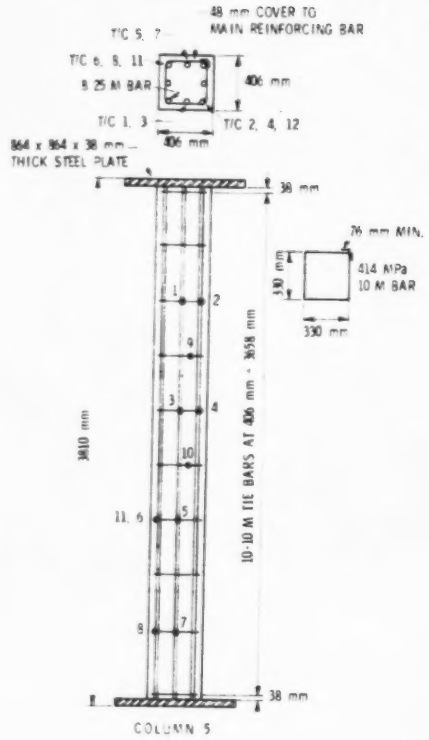

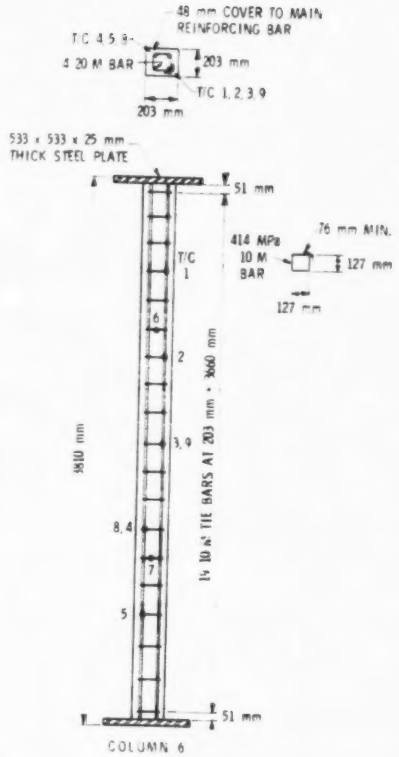

FIGURE 5
THERMOCOUPLES ON REINFORCING BARS

BR 6432-5

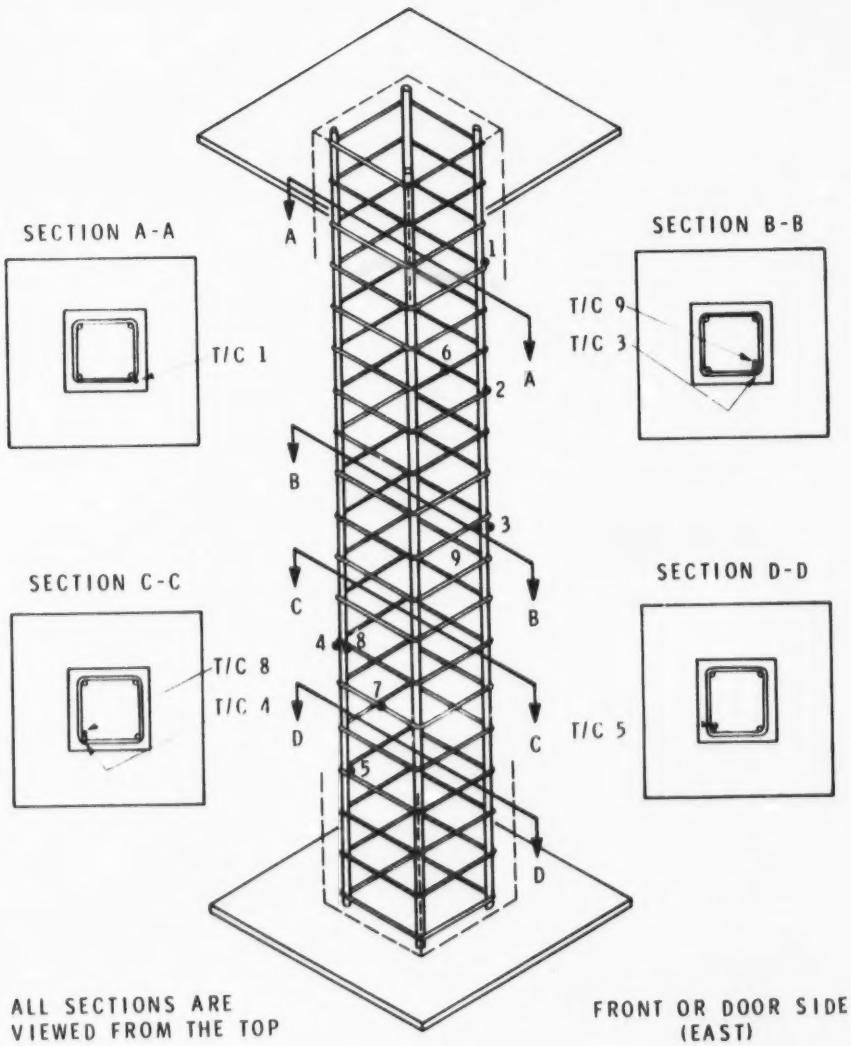

FIGURE 6

THERMOCOUPLES ON REINFORCING BARS (203 x 203 mm COLUMN)

BR 6446-5

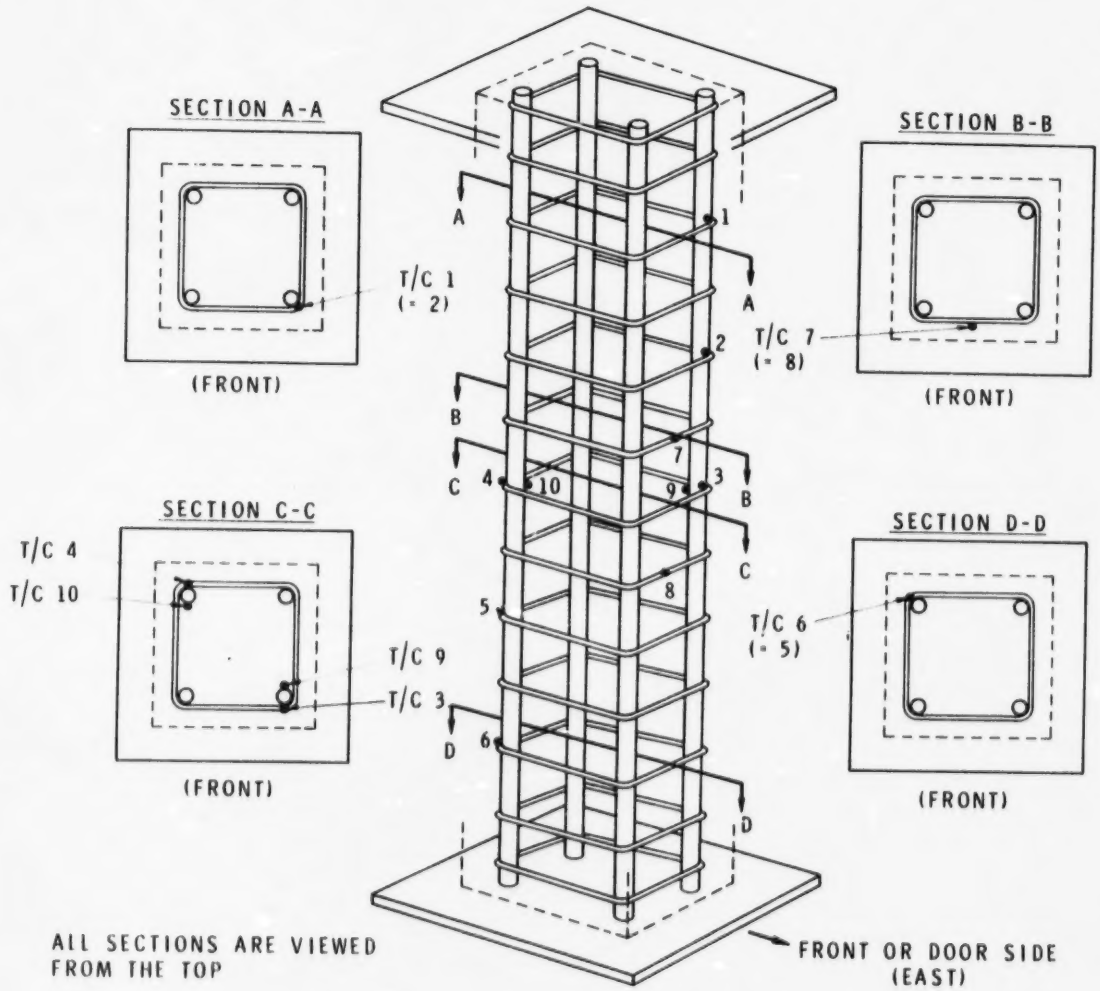

FIGURE 7

THERMOCOUPLES ON REINFORCING BARS (305 mm x 305 mm COLUMN)

BR 6432-6

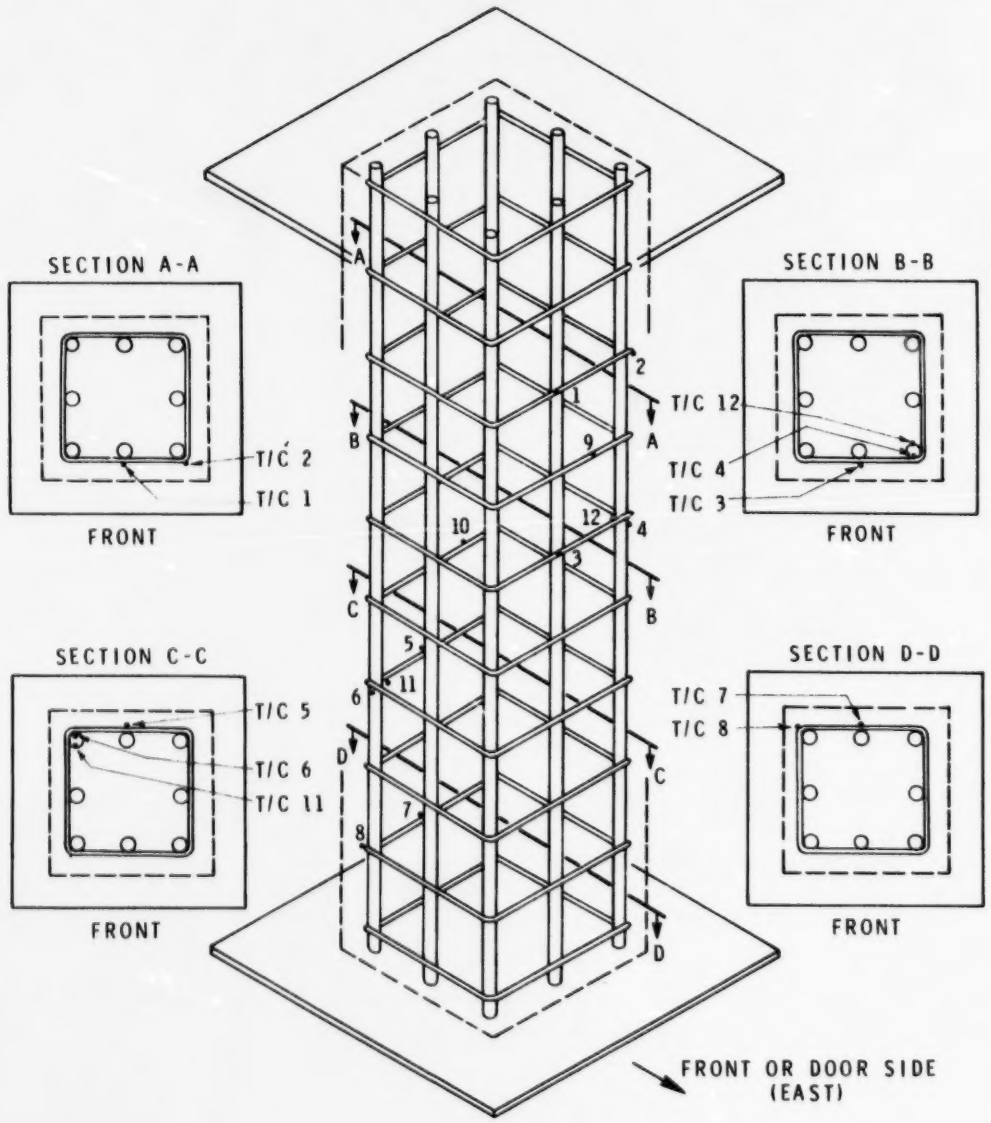

FIGURE 8
THERMOCOUPLES ON REINFORCING BARS (406 mm x 406 mm COLUMN)

BR 6441-5

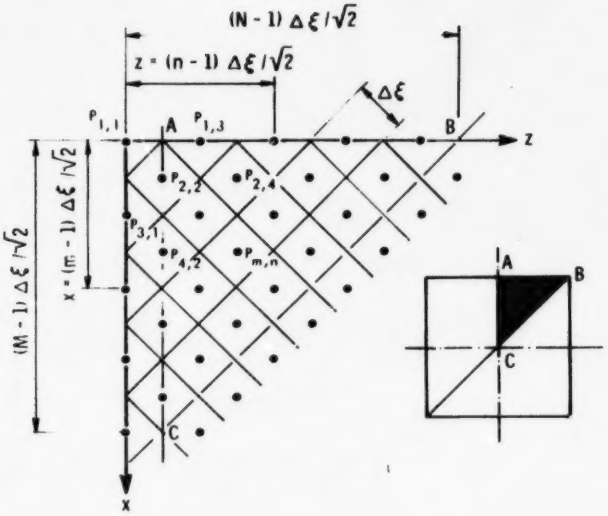

FIGURE 9

TRIANGULAR NETWORK OF ELEMENTS IN A ONE-EIGHTH SECTION OF COLUMN

BR 6477-1

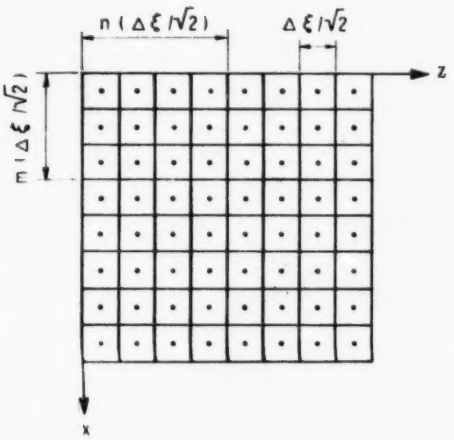

FIGURE 10

SQUARE NETWORK OF ELEMENTS IN A QUARTER SECTION OF COLUMN

BR 6477-2

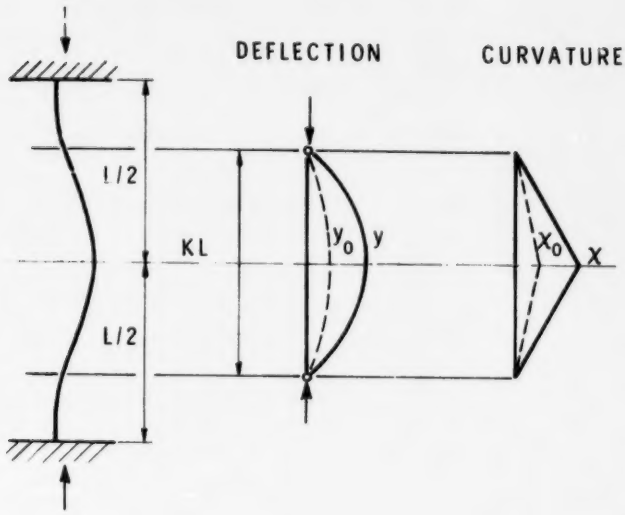

FIGURE 11
LOAD-DEFLECTION ANALYSIS

BR 6477-3

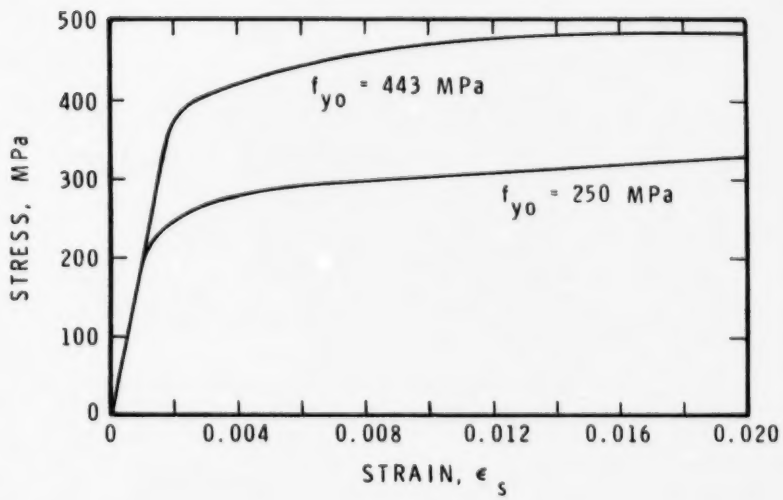

FIGURE 12
STRESS-STRAIN CURVES FOR TWO STEELS AT 20°C

BR 6477-4

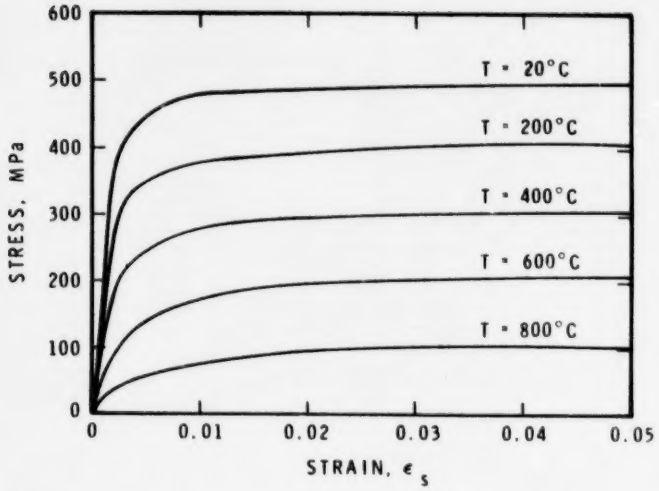

FIGURE 13

STRESS-STRAIN CURVES FOR THE REINFORCING STEEL AT VARIOUS TEMPERATURES (f_{yo} = 443 MPa)

BR 6477-5

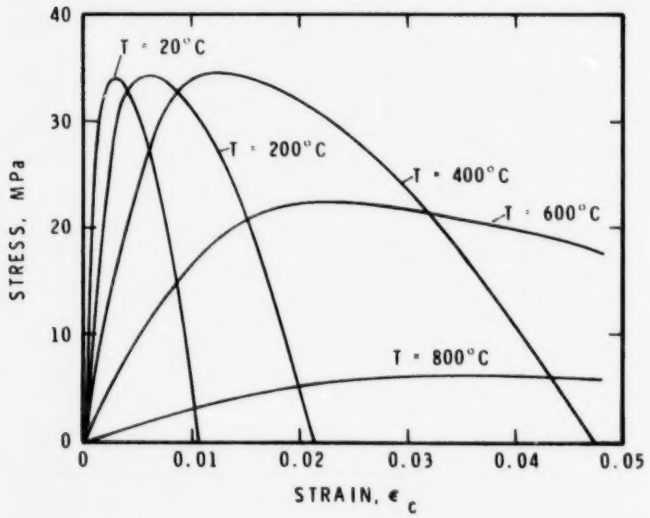

FIGURE 14

STRESS-STRAIN CURVES FOR CONCRETE AT VARIOUS TEMPERATURES (f'_{co} = 35 MPa)

BR 6477-6

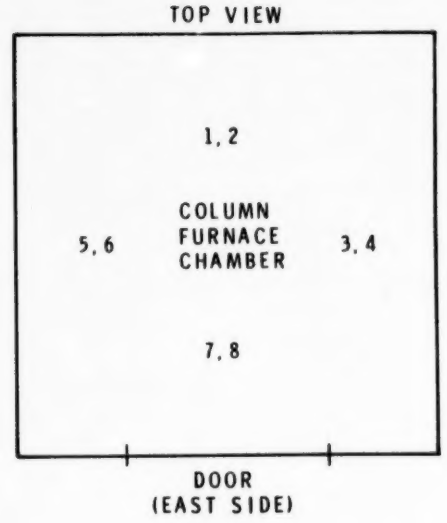

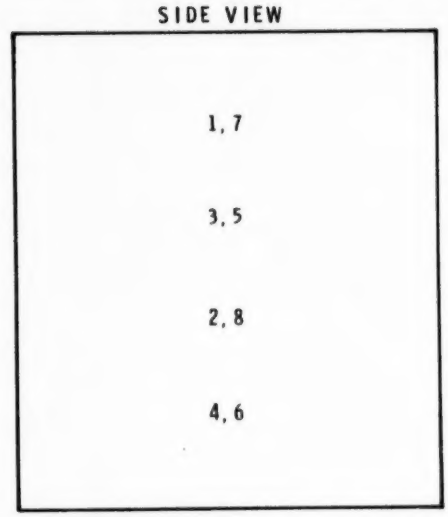

FIGURE 15

LOCATION AND NUMBERS OF THERMOCOUPLES IN COLUMN FURNACE CHAMBER

BR 6432-7

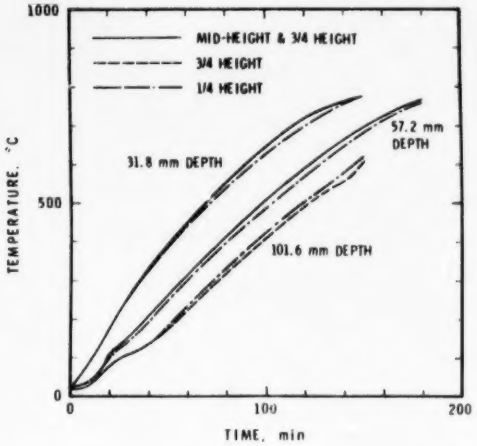

COLUMN NO. 6
SECTION: 203 x 203 mm

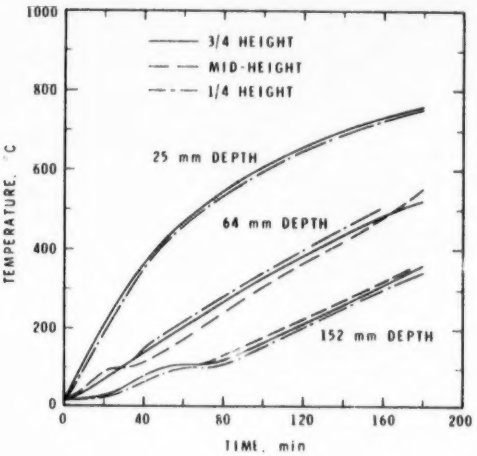

COLUMN NO. 1
SECTION: 305 x 305 mm

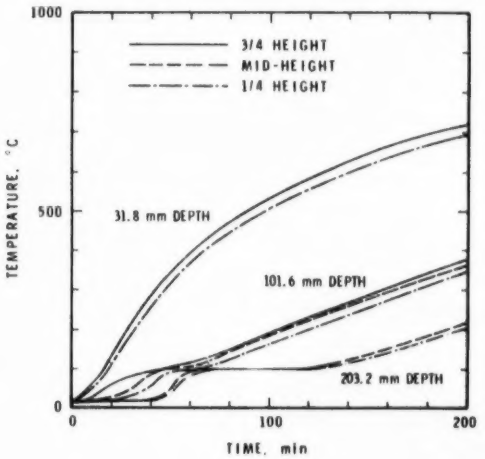

COLUMN NO. 5
SECTION: 406 x 406 mm

FIGURE 16

TEMPERATURES MEASURED IN CONCRETE SECTION ALONG CENTRELINE AT VARIOUS DEPTHS AND COLUMN HEIGHTS

BR 6441-8

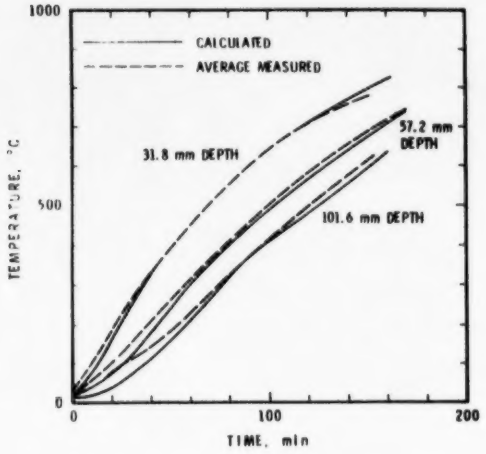

COLUMN NO. 6
SECTION: 203 x 203 mm

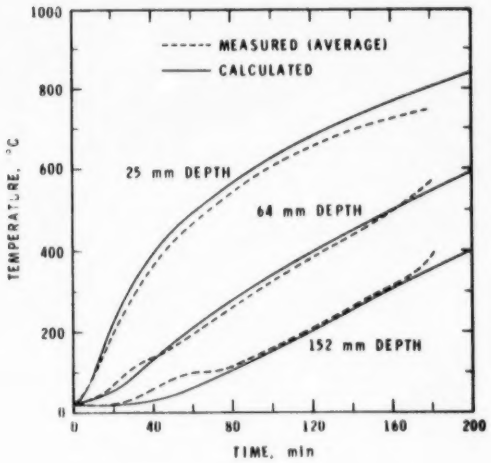

COLUMN NO. 1
SECTION: 305 x 305 mm

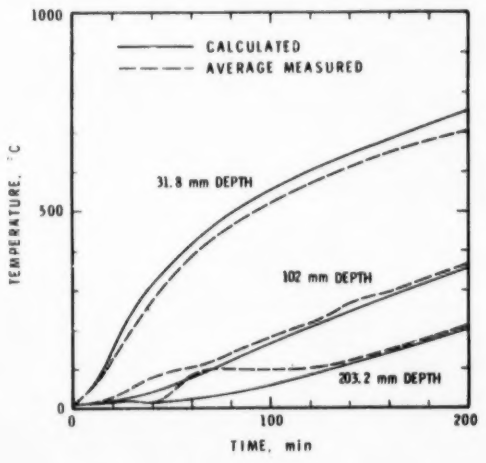

COLUMN NO. 5
SECTION: 406 x 406 mm

FIGURE 17

CONCRETE TEMPERATURES IN SECTION ALONG CENTRELINE AT VARIOUS DEPTHS

BR 6441-9

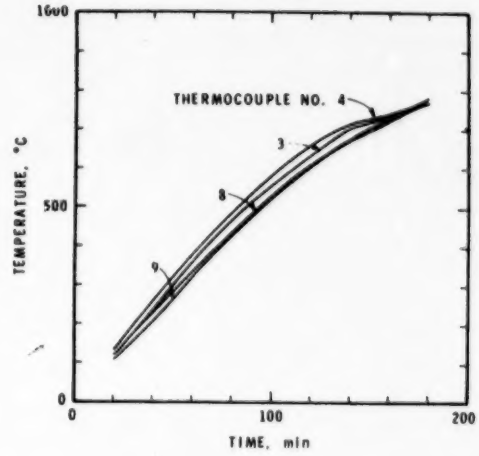

COLUMN NO. 6
SECTION: 203 x 203 mm

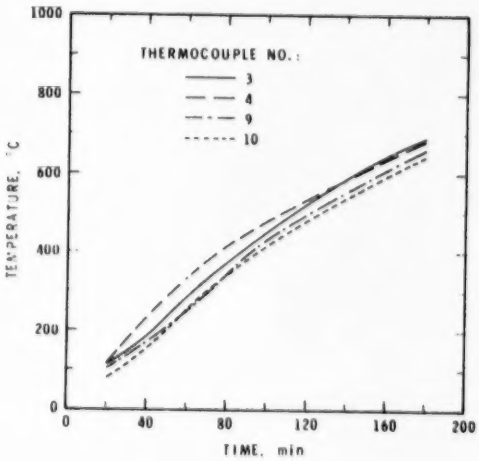

COLUMN NO. 1
SECTION: 305 x 305 mm

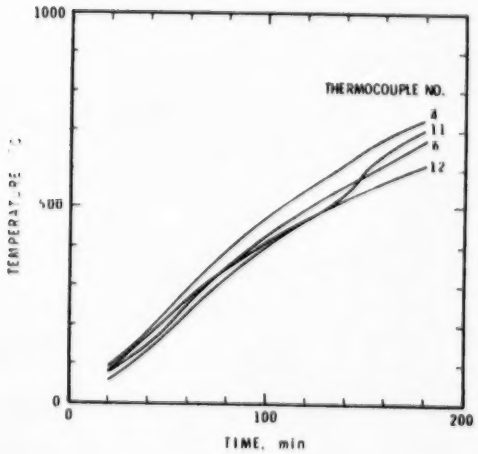

COLUMN NO. 5
SECTION: 406 x 406 mm

FIGURE 18

TEMPERATURES MEASURED ON MAIN REINFORCING BARS

BX 6441 /

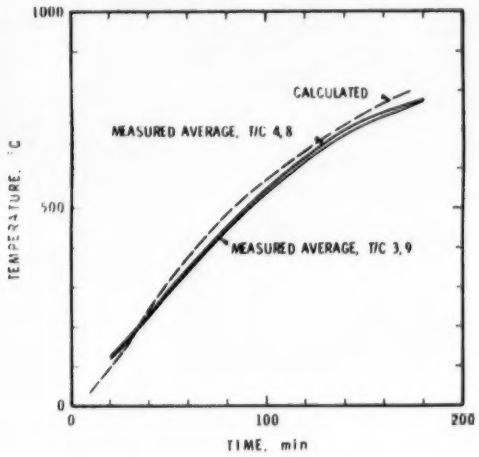

COLUMN NO. 6
SECTION: 203 x 203 mm

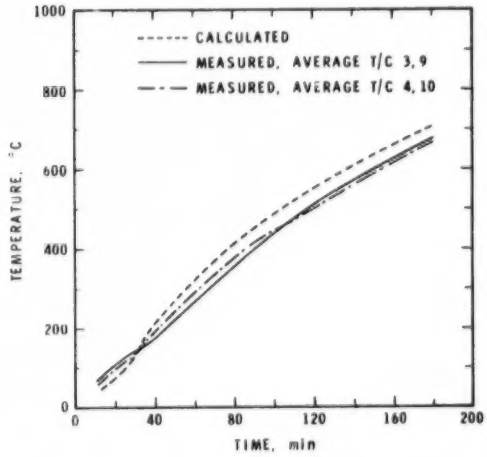

COLUMN NO. 1
SECTION: 305 x 305 mm

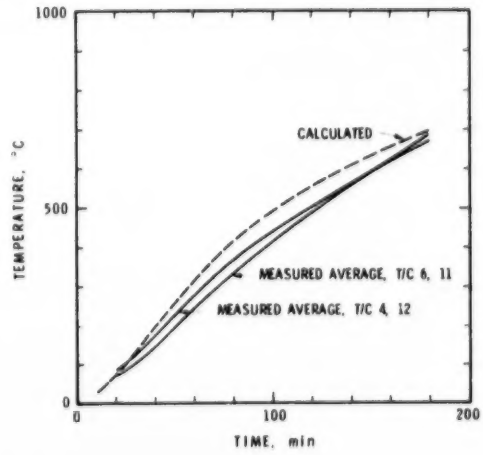

COLUMN NO. 5
SECTION: 406 x 406 mm

FIGURE 19

CALCULATED AND MEASURED AVERAGE TEMPERATURES OF MAIN REINFORCING BARS

BR 6441-6

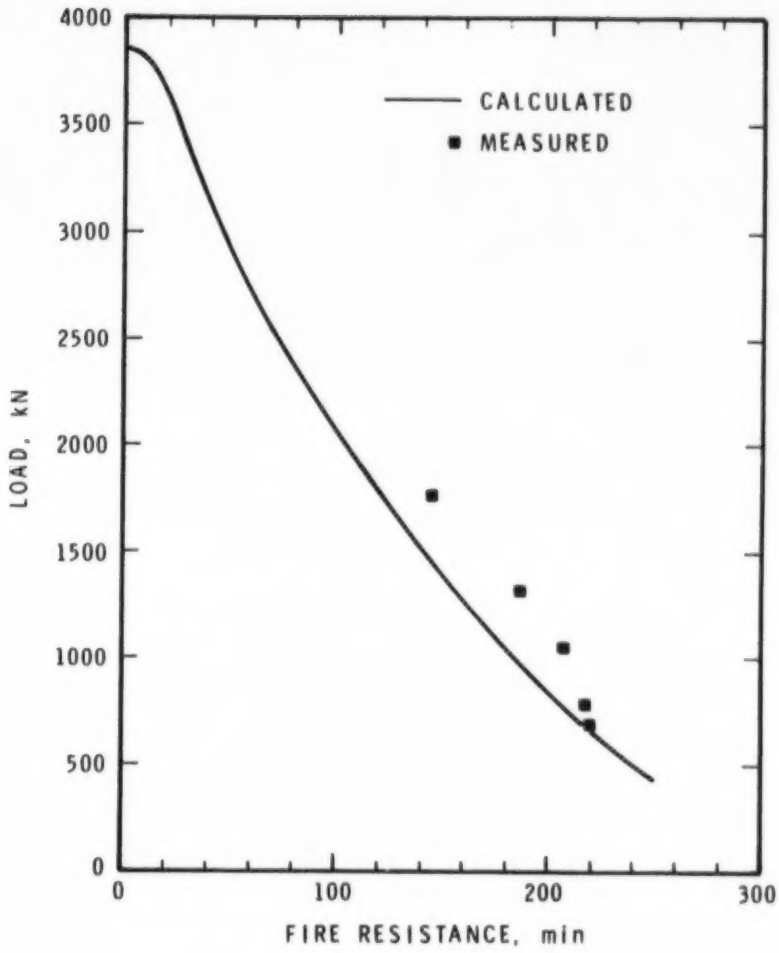

FIGURE 20

INFLUENCE OF LOAD ON FIRE RESISTANCE
(305 x 305 mm SECTION SIZE)

BR 6477-7

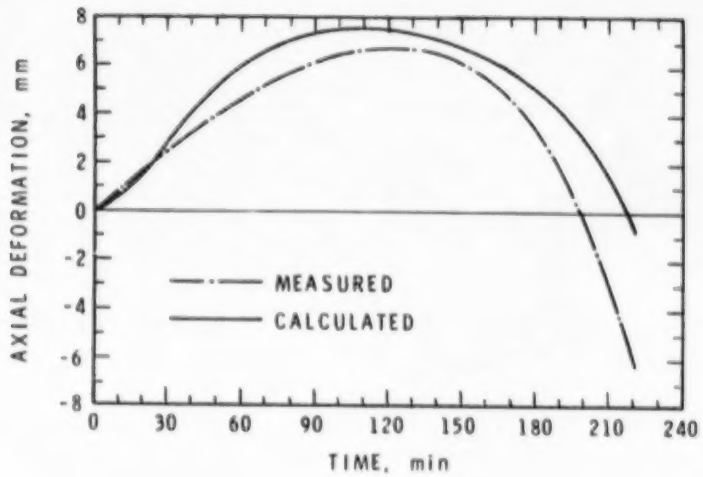

FIGURE 21

AXIAL DEFORMATION AS A FUNCTION OF TIME
(LOAD: 800 kN (180 kips))

BR 6424-7

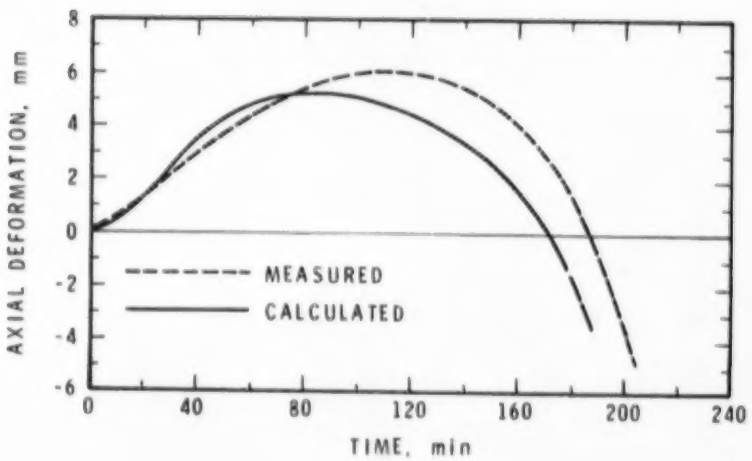

FIGURE 22

AXIAL DEFORMATION AS A FUNCTION OF TIME
(LOAD: 1067 kN (240 kips))

BR 6455-6

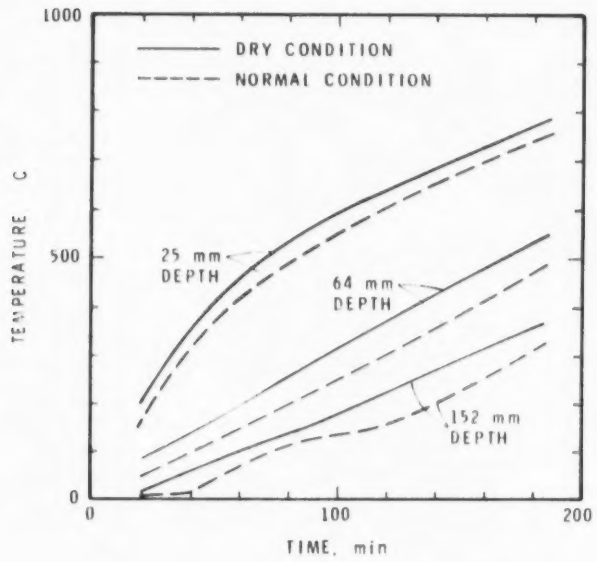

FIGURE 23

INFLUENCE OF MOISTURE ON CONCRETE TEMPERATURES (MEASURED IN MID-HEIGHT SECTION ALONG CENTERLINE)

BR 6477-8

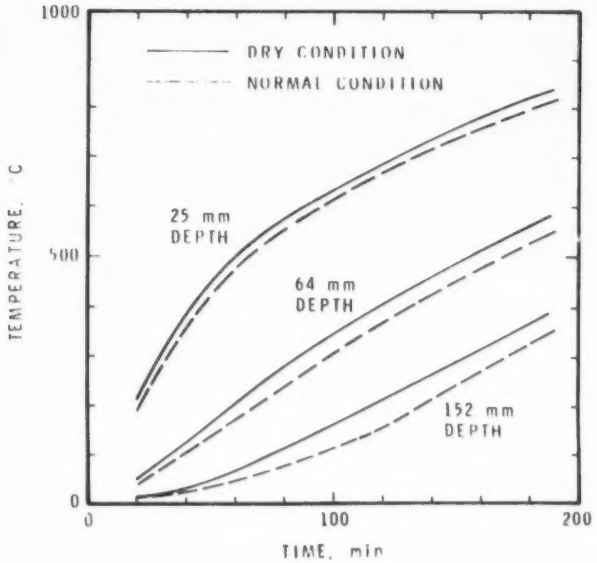

FIGURE 24

INFLUENCE OF MOISTURE ON CONCRETE TEMPERATURES (CALCULATED FOR SECTION ALONG CENTERLINE)

BR 6477-9

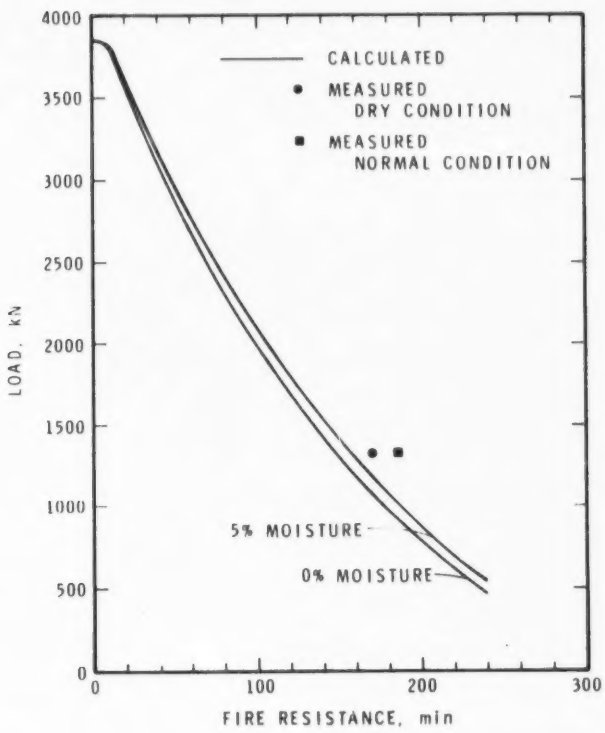

FIGURE 25
INFLUENCE OF MOISTURE ON FIRE RESISTANCE

BR 6477-10

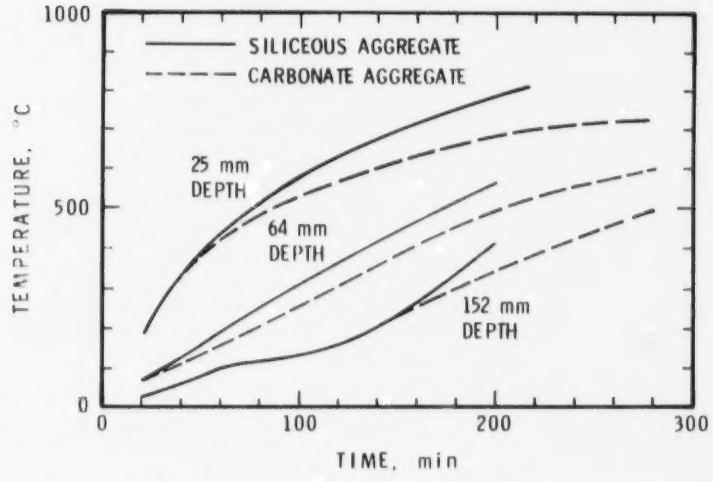

FIGURE 26

INFLUENCE OF AGGREGATE ON TEMPERATURES IN COLUMN (MEASURED IN MID-HEIGHT SECTION ALONG CENTERLINE)

BR 6477-11

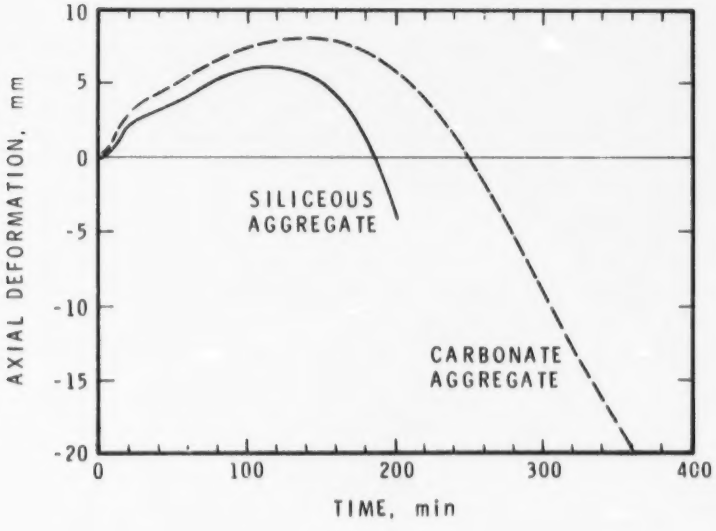

FIGURE 27

INFLUENCE OF AGGREGATE ON AXIAL DEFORMATION OF COLUMN

BR 6477-12